IR spectroscopy of alkali halides at very high pressures: Calculation of equations of state and of the response of bulk moduli to the $B1$-$B2$ phase transition

A. M. Hofmeister
Department of Earth and Planetary Science, Washington University, St. Louis, Missouri 63130
(Received 30 January 1997)

New infrared (IR) data on NaF, NaCl, KCl, KBr, and KI were obtained at pressures of up to 42 GPa. The large ($\sim$20%) drops in vibrational frequencies of alkali halides upon transformation of the $B1$ phase to $B2$ are due to the decrease in bond strength as ionic separation increases, and strongly suggest that the bulk modulus K_T generally *decreases* during the transition, rather than increases, as commonly accepted. Bulk moduli and equations of state for $B1$ phases are obtained from one initial volume V_0 and our vibrational frequencies $\nu_i(P)$ using a semiempirical model (previous IR data are used for Rb halides). For substances with a cation radius that is greater than 0.6 times the anion radius, initial values K_0 are within 0.4 to 5% of ultrasonic determinations: thus, this model is accurate for cases where quantum mechanical calculations falter. The converse holds for relatively small cations. Curvature of K_T with pressure matches the previous determinations even if K_0 is not precisely predicted, which allows determination not only of K_0', but also of K_0'', which is generally poorly constrained. Care must be taken in specifying the equation of state, as values for both K_0' and K_0'' are affected by the format chosen. For the $B2$ phases, $V(P)$ and $K_T(P)$ are constrained through similar calculations which utilize the volume at the transition as the starting point. Our results are unaffected by shear stress, in contrast to previous x-ray determinations for $B2$. After transformation at 32 GPa, K_T of NaCl-$B2$ is 119 ± 4 GPa, 16 ± 3% *below* that of $B1$. $K_T(P)$ of $B2$ rises steadily (K' is fairly large, 4.7 ± 0.3) resulting in a λ curve. Results derived for KCl, KBr, and KI are similar such that $K(P)$ of their $B2$ phases are better constrained than those of $B1$ due to larger stability fields. For the Rb halides, K_T is roughly constant across the phase change. The compositional dependence of the changes in frequency, K_T, and V for alkali halides are compatible with a simple ball-and-spring model. The calculated $B2$ phase volumes of the Na halide are infinite at 1 atm, consistent with instability below 8 GPa, which suggests that theoretical calculations should avoid use of 1 atm starting points for the high-pressure $B2$ phases. [S0163-1829(97)07134-8]

INTRODUCTION

One of the simplest pressure-driven reconstructive phase transitions is that converting the rock salt structure (the $B1$ phase) to the CsCl structure (the $B2$ phase) during which the coordination changes from 6 to 8. Understanding this system is a precursor to modeling pressure driven phase transitions in complex solids. Several studies used quantum mechanics to model equations of state (EOS); however, predictions of bulk modulus K_T err as much as 15 to 25% (see Refs. 1 and 2, and citations therein). Data critically needed to test the models, such as the change in bulk modulus K_T across the transition, are poorly constrained (Recio *et al.*[1]), despite the existence of numerous measurements of macroscopic properties of alkali halides, e.g., Refs. 3–11. For example, it is generally accepted that the bulk modulus increases across the transition,[12] and increases have been calculated (e.g., Ref. 2) and inferred mainly from $V(P)$ data (e.g., Refs. 4–8). Yet, a *decrease* in K_T at the transition was recently predicted theoretically for LiCl and NaCl,[1] calculated semiempirically,[13] and indicated by experimental measurements of the acoustic modes of KBr and KI,[9] and by high-accuracy piston-cylinder measurements of ΔK for the K halides and RbCl.[10] The controversy[10] arises mainly because $B2$ volumes cannot be measured at 1 atm: hence, the three parameter description of the $B2$ data (V_0, K_0, K_0') derived from volume[5–7] is fraught with uncertainty (see discussion in Ref. 5). Additional errors in $V(P)$ are incurred through the use of solid-pressure transmitting media,[14] which lead to overestimation of the bulk moduli.[15] Acoustic data[8] only yield compression velocities v_p, hence, calculation of K_s not only requires assumption of V_0 and K_0' with the resulting K_s being highly dependent on the chosen equation of state,[8] but also assumes proportionality of shear velocity to v_p. The latter assumption[8] is counterindicated by data on acoustic velocities.[9] Ultrasonic determination of K_s for the $B2$ phases[4] is also problematic: as discussed by Shaw,[4] the ultrasonic data are affected in an indeterminate way by the change in length during transformation. Occurrence of hysteresis during the transition[5,6,11] adds ambiguity to all these studies and high transformation pressures for sodium halides compound the experimental difficulties. Improvements in theoretical methodologies and additional experimental approaches are needed, as previously discussed.[1,16]

Well-constrained measurements of phonon frequencies ν_i over a wide range in pressure not only provide a rigorous test for theoretical models, but moreover such data can be used in semiempirical models, e.g., Refs. 17–18, to give parameters such as the change in K_T across the transition. Existing spectral data are limited to <3 GPa,[9,19–22] many of the measurements were made without gaskets[19,20] and all lack internal pressure calibration, hence, data across the $B1$-$B2$ transition exist for RbBr, RbI, KBr, and KI, but $\nu_i(P)$ may not be accurate.

This study presents far-IR measurements of NaCl to 42 GPa, of KBr and KI to 35 GPa, and of NaF and KCl to 23 GPa. The pressure dependence of the bulk modulus $K_T(P)$ is derived from a modified Blackman/Brout model[17–18] for both $B1$ and $B2$ phases. The motivation is (1) to constrain K_0'', which is ill constrained by compression data as it is a third derivative and small in magnitude, and ultrasonic experiments infrequently reach sufficiently high pressure to establish K'' accurately, (2) to quantify the change in K_T across the transition, (3) to determine EOS parameters for the $B2$ phases which do not require assuming a value for V_0 or K', and (4) to calculate the mode Grüneisen parameters and their derivatives (in a companion paper). For moderately large cations ($r_c/r_a > 0.6$ where r is the ionic radius), the accuracy for the $B1$ phases is ± 0.5 GPa or better if the zero point correction is considered, which compares favorably with experimental limitations and is more accurate than recent theoretical results.[1,2] Bulk moduli for $B2$ phases at the transition are calculated for RbBr and RbI from existing spectroscopic data[19–22] and for RbCl and NaF by interpolating frequencies. A new equation of state (EOS) is derived for the $B2$ phases which neither requires 1 atm values as inputs nor is affected by shear stress. Our results corroborate the *decrease* in K_T across this transition observed by Boehler and Zha[10] and predicted for NaCl by Recio *et al.*[1] A simple model proposed for these materials accounts for the compositional dependence of the physical properties. Our calculated EOS points to an infinite volume for the $B2$ phase of NaCl at 1 atm, suggesting that (1) models of the $B2$ phases of Na and Li halides should focus on properties at the transition pressure rather than at 1 atm, and (2) elasticity data for $B2$ phases have not been properly extracted from compressibility measurements.

EXPERIMENTAL

High-purity alkali halides (99.9%) were compressed at room temperature with a Mao-Bell-type diamond cell[23] in a sandwich configuration: a thin film of sample was formed on the piston diamond, ruby film was sprinkled on the cylinder diamond and the gasket aperture of ~300 mm was filled with petroleum jelly (run Nos. 1 and 5) or high density polyethylene. Run No. 4 utilized a 0.15 mm aperture and petroleum jelly, and had a thick (several μm) film of NaCl. The film in run No. 1 was about 1 μm thick; all others were submicron thicknesses. Run No. 5 also contained a thin film of high purity KI. Run No. 6 contained films of NaF and KCl and used a 0.10 mm aperture. Run No. 7 contained KBr and the spinel phase of Mg_2SiO_4 and used a 0.11 mm aperture. Type-I diamonds with ~0.33 carat weight and 0.6 mm diameter flat tips were used. Pressure was determined using the ruby fluorescence technique using an automated scanning spectrometer.[23] (Subsequent revisions in the ruby scale pertain only to pressures considerably larger than those measured here.) For run Nos. 4 and 5, more than 80 measurements of the R_1 line in a grid across the surface were taken. For run Nos. 1, 6, and 7, roughly 50 points were sampled. For run Nos. 2 and 3, about ten points were sampled. Average pressure is reported; uncertainty is determined from statistics. For NaCl at 20 GPa, the pressure gradient across the cell was <5 GPa, whereas at 40 GPa, the gradient was <10 GPa. For NaF, KCl and KBr, use of a small sample chamber reduced the pressure gradient by at least half.

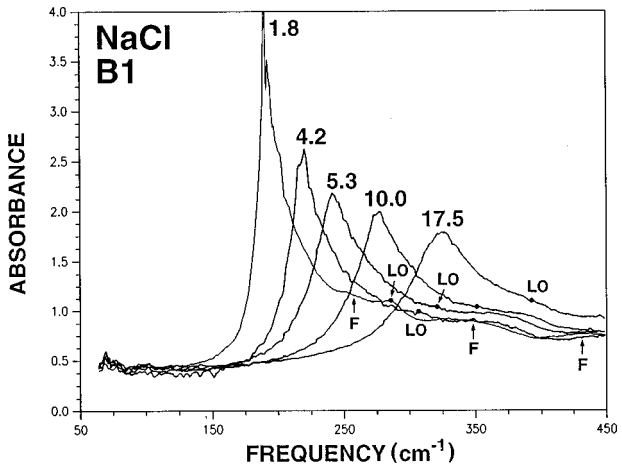

FIG. 1. Far-IR spectra of NaCl with the $B1$ structure at various pressures. Spectra are labeled with pressures in GPa. This series comprises the data from experiment No. 1 taken during decompression. Solid dot: LO peak positions, F: interference fringes.

Spectra were acquired at 4 cm^{-1} resolution in a purged Nicolet 7199 Fourier-transform infrared (FTIR) spectrometer equipped with a liquid-He-cooled Si bolometer and a 6 μm Mylar beam splitter, over frequencies of 70–480 cm^{-1}. Throughput was enhanced fourfold with a beam condenser.[24] Spectra were collected during compression and decompression except for run No. 4 which was terminated by a diamond shattering. Typical run conditions were 2000–2500 scans with a gain of 64–128 and a mirror velocity of ~0.56 cm/s. Reference spectra were collected from an empty, ungasketted diamond-anvil cell (DAC). Slight differences in humidity cause traces of the water-vapor rotational bands[25] to be present as small, sharp peaks from 100–305 cm^{-1}. These peaks were not subtracted because they did not interfere with the intense, broad alkali halide absorption bands.

The spectra are dominated by the intense transverse optic (TO) band (Figs. 1 and 2). The weaker longitudinal optic (LO) mode is present due to the oblique incidence of the light traversing the DAC and to the fact that the films are ''thick'' and may be wedged.[26] Thus the LO modes are not well-constrained, but the most reliable data are included for completeness.

SPECTROSCOPIC RESULTS

Pressure dependence of the B1 IR modes in NaCl. The thin-film spectrum at 1 atm has a strong peak at 164 cm^{-1} which matches the TO position obtained from the reflectance spectrum of single-crystal NaCl at ambient conditions, and a weak peak at 257 cm^{-1} which is slightly offset from the LO component at 264 cm^{-1}. Peak positions increase nonlinearly with pressure up to the reconstructive transformation near 32 GPa (Figs. 1 and 2). The positive shift is in accord with shortening of bond lengths as pressure increases, and its continual decrease with pressure is in accord with increasing resistance of the bonds to compression.

The TO mode is constrained by 36 data points which span

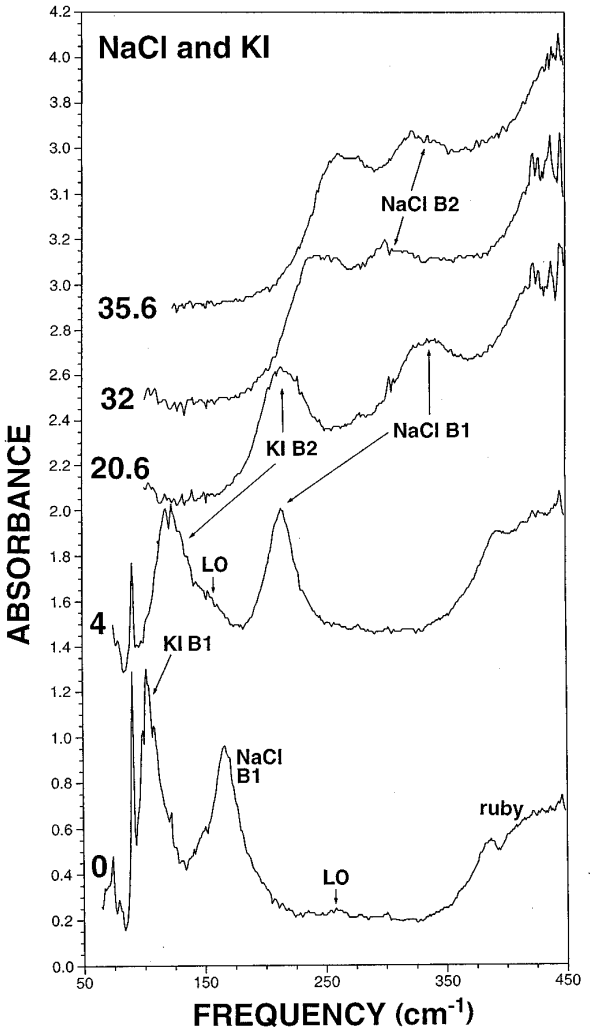

FIG. 2. Far IR of NaCl and KI at various pressures (experiment No. 5). Spectra are offset for clarity and labeled with pressures in GPa. The baseline at the lowest frequencies measured is at about 0.2 absorbance units for each spectrum. Peaks due to ruby occur from 360 to 450 cm^{-1} at ambient pressure and shift to $>425\ cm^{-1}$ by 35 GPa. The TO peaks are labeled according to chemistry and structure. The 32 GPa pressure is an estimate: this datum was not included in the analysis.

the stability range of $B1$ (Table I). Peak positions are listed sequentially in order to differentiate decompression from compression runs. Although strong curvature of $\nu_{TO,B1}$ with pressure is seen [Fig. 3(a)], our initial slope of 15.4 cm^{-1}/GPa equals that previously obtained below 0.62 GPa.[21]

The LO component could not be traced in all spectra due to its weakness. Channel fringes are also present and spaced at roughly 80 cm^{-1} (Figs. 1 and 2). This sinusoidal baseline cannot be intrinsic to the sample because it is also seen in the reference spectra, as shown in Ref. 24. Positions of the artifacts are unaffected by pressure, allowing LO peaks to be differentiated by their pressure dependence. LO modes for $B1$ most prominent for the thick films of series No. 1 and No. 4, yielding 20 different data points (Table I). The trend of the LO mode for $B1$ with pressure is roughly parallel to that of the TO mode [Fig. 3(a)], although the LO-TO split-

TABLE I. (a) Vibrational data on NaCl in the $B1$ structure at pressure (b) NaCl infrared series with partial conversions. (c) Infrared data on NaCl loaded with KI (series No. 5). (d) Infrared data on NaF loaded with KCl (series No. 6). (e) KBr in the $B2$ phase (series No. 7).

Expt. No.	Pressure GPa	ν_{LO} cm^{-1}	ν_{TO} cm^{-1}
	(a)		
1-$B1$	5.8±0.2	329	234
	9.4±0.8	370±5	262
	17.5±1.5	392±4	321
	10±1	350	274
	8.1±0.8		263
	5.3±0.5	328	240.3
	4.2±0.4	308	217.1
	1.8±0.2	282	190.8
2-$B1$	7±1	338±5	245
	10.5±1		288
	17.5±2.5		330±6
	20.5±2.5		340±6
3-$B1$	2.5±0.5	310±5	207
	6.5±1		241
	11±1		289
	16±2		319
	13±1.5		305
	9.3±1		276
	3.8±0.5	295±5	224±2
	0.9±0.2	272	177

(b)

	$B1$ area			$B2$ area		
Expt. No.	Pressure GPa	ν_{LO} cm^{-1}	ν_{TO} cm^{-1}	Pressure GPa	ν_{LO} cm^{-1}	ν_{TO} cm^{-1}
4-$B1$+$B2$	23±1	433±5	350±5			
	27.7±1.5		375±5			
	27.6±1[a]	446±5	375±5	34±1[a]		297±1
	30±0.5[a]	448±5	382±5	36.5±1.0[a]		310±2
	32.2±0.2[a]	450±2	390±5	38.5±1.0[a]	425±5	330±10
				40±1	432±5	350±8
				42.3±0.6	450±5	366±6

(c)

	NaCl					
Pressure GPa	Phase	ν_{LO} cm^{-1}	ν_{TO} cm^{-1}	Phase	ν_{LO}[b] cm^{-1}	ν_{TO} cm^{-1}
6.5±0.1	$B1$		238	$B2$		149.2
13.3±0.2		360±5	294			185
19.0±0.3		413	332			211
22.9±0.4			354			224.4
27.2±0.8			374			
28.5±0.5	mixture					239.3
34±1	$B2$		301			
35.6±0.6			325±2			264
35.3±0.5		375±5?	318±2			256.4
29.8±0.4	mixture					241
20.6±0.4	$B1$		336			213
4.0±0.1			212		150	119
2.2±0.1			192.8		137±5	103.4
0		257	164.7	$B1$	139	100.1
1.0±0.1		274	174.4		156	114
1.3±0.1		277	182.3		165	120

TABLE I. (*Continued*).

(d)

	NaF		KCl		
Pressure GPa	ν_{LO} cm^{-1}	ν_{TO} cm^{-1}	Phase	ν_{LO}[c] cm^{-1}	ν_{TO} cm^{-1}
4.4±0.1	444	295.4	*B*2	236	162±2
9.3±0.1	480	333		263	210
17.4±0.1		380.4		306	258±2
22.8±0.2		412		~330	277
20.8±0.2		404		316	271
11.1±0.2		346.7		275	222.7
4.9±0.1		295.4		241	172
1.8±0.1[a]				215	145
1.5±0.1	419	268.2			
1.4±0.1[a]			*B*1		159
0.4±0.1	417	253.3		224.4	149
1.7±0.1	426	270		248	163.9
2.3±0.1	425	273.5			169
2.7±0.1					173.6
2.8±0.1	431	277			
3.1±0.1			*B*2		153

(e)

Pressure GPa	ν_{TO} cm^{-1}
11.60±0.05	174
16.2±0.2	204
23.7±0.4	241
28.5±0.5	259
35.9±0.6	282

[a]These pressures were determined by assuming that pressure from the center of the cell corresponded to the *B*2 phase and that the presures near the edge corresponded to the *B*1 phase. The areas for *B*1 and *B*2 phases were assumed to be equal, for simplicity.
[b]Most LO modes of KI were obscured by the NaCl peaks.
[c]Some LO modes of KCl were obscured by the NaF peaks.

ting may decrease from 100 cm^{-1} at ambient pressure to 60 cm^{-1} at 32 GPa.

A high-order polynomial with pressure best describes the observed changes in frequencies upon compression (Table II). Other functions (exponentials and logarithms in volume or pressure) fit the data less well. Mode Grüneisen parameters, $\gamma_{i_0}=K_{T_0}(d\nu_i/dP)_0/\nu_{i0}$, calculated for the *B*1 phases using ultrasonic data for K_{T_0},[27–34] are roughly 2 for the TO modes and 1 to 1.6 for the LO component.

Other peak parameters are also affected by pressure. Peak width and area increase and intensity decreases as pressure increases (Fig. 1), such that the oscillator strength decreases slightly with pressure. This may be intrinsic, as a weak decrease in oscillator strength is consistent with the observed weak dependence of the LO-TO splitting on pressure [Fig. 3(a)].

Pressure dependence of the B2 IR modes in NaCl. Peaks for *B*2 phase are broad (Fig. 2), possibly due to the larger pressure gradient found at high pressure. This reconstructive transformation causes a significant drop in frequency,

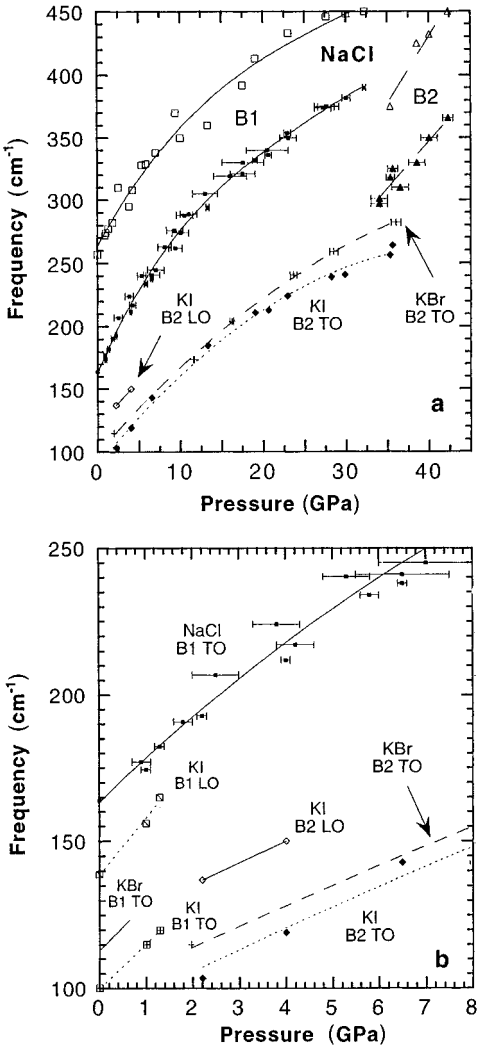

FIG. 3. Pressure dependence of alkali halide IR modes. (a) High pressure data on NaCl and the B2 phases of KI and KBr. Small filled squares: TO modes of NaCl in the B1 phase; open squares: LO of NaCl with the B1 structure; filled triangles: TO of NaCl-B2; open triangles: LO of NaCl-B2; filled diamonds, TO of KI with the B2 structure; open diamonds: LO of KI-B2; plus sign: KBr-B2. All lines are least squares fits of polynomials or linear fits in pressure to the data (Table II). (b) Low pressure data on KI, KBr, and NaCl. Square with cross: the TO mode of KI in the B1 structure; square with slash: LO of KI-B1; solid line: KBr-B1 data from Ref. 21.

~100 cm^{-1} (Table I; Figs. 2 and 3) due to the increase in bond length required for an increase in the number of nearest neighbors, see discussion section. *B*2 modes change linearly with pressure over the measured interval but with a steeper slope than that seen for *B*1 (Table II), and the LO-TO splitting appears to increase rather than decrease, in contrast to the behavior of *B*1. The linear dependence and increase in the LO-TO splitting are artifacts attributed to the narrow range of pressures attained for *B*2, to the lower accuracy in *P* due to the increased pressure gradient, and to difficulty in tracing the LO mode of the *B*2 phase. Probably, the LO mode parallels the TO mode within this pressure range, as suggested by the three highest pressure points for the LO mode [Fig. 3(a), Table II], and as occurs for KCl (see below).

TABLE II. Polynomial representations of the pressure dependence of the IR modes of alkali halides and their Grüneisen parameters.

Mode	ν (in cm^{-1} with P in GPa) [a]	$\gamma_{i_0}(B1)$ [b]
NaF $B1$TO	$246.893+10.902P-0.1651P^2$	2.04
NaF $B1$LO	$412.968+7.080P$	0.79
NaCl $B1$TO	$164.676+15.489P-0.5350P^2+0.01212P^3-0.0001127P^4$	2.25
NaCl $B1$LO	$263.5122+12.1427P-0.30196P^2+0.0034031P^3$ [c]	1.10
NaCl $B2$TO	$42.756+7.6129P$	
NaCl $B2$LO	$5.0543+10.646P$ [d]	
KCl $B1$TO	$142.652+13.415P-0.7648P^2$	1.63
KCl $B1$LO	$215.11+19.55P$	1.57
KCl $B2$TO	$119.936+11.397P-0.198P^2$	
KCl $B2$LO	$205.213+7.1282P-0.0781P^2$	
KBr $B1$TO	$114.0+15.9P$ [f]	2.01
KBr $B1$LO	$165.0+15.9P$ [e]	1.39
KBr $B2$TO	$97.876+7.624P-0.0693P^2$	
KBr $B2$LO	$148.876+7.624P-0.0693P^2$ [e]	
KI $B1$TO	$100.3+15.224P$ [h]	1.74
KI $B1$LO	$138.6+19.262P$	1.60
KI $B2$TO	$78.825+11.613P-0.3228P^2+0.00393P^3$	
KI $B2$LO	$121.13+11.613P-0.3228P^2+0.00393P^3$ [e]	
RbCl $B1$TO	$116+16.3P$ [f]	2.18
RbCl $B1$LO	$173+16.3P$ [e]	1.47
RbBr $B1$TO	$87.5+16.3P$ [f]	2.42
RbBr $B1$LO	$127+16.3P$ [e]	1.67
RbBr $B2$TO	$74+21P$ [f]	
RbBr $B2$LO	$105+21P$ [e]	
RbI $B1$TO	$75.5+14.8P$ [f]	1.97
RbI $B1$LO	$103.0+14.8P$ [e]	1.44
RbI $B2$TO	$70.0+4.0P$ [g]	
RbI $B2$LO	$97.5+4.0P$ [e]	

[a]Transition pressures are 32 GPa for Na halides, 1.9 GPa for K halides, and 0.5 for Rb halides.
[b]Calculated using ultrasonic measurements for K_0 (Refs. 25–32).
[c]Initial slope is poorly constrained: a linear fit to the first four data points gives 15.9 cm^{-1}/GPa.
[d]This trend is defined by all four data points. Three data points fall on a trend of $166.55+6.6833P$: because this results in the LO-TO splitting being nearly constant and slightly decreasing, as observed for $B1$, the lowest pressure point is probably inaccurate, and the latter trend is used to determine γ_{i_0}.
[e]LO-TO splitting is assumed const = 38 cm^{-1} for KI $B2$; 40 cm^{-1} for RbBr $B1$ or $B2$; and 51 cm^{-1} for KBr and 27.5 for RbI (see text).
[f]Data from Lowndes and Rastogi (Ref. 21).
[g]Data from Ferraro *et al.* (Ref. 20). The frequency at the transition is accurate, but the slope is uncertain (see text).
[h]The initial slope was taken from the lower pressure data of Ref. (21) is 18.8.

Pressure Dependence of the KI modes. Initial values of 100 and 139 cm^{-1} for the IR modes of KI match those obtained from single-crystal reflection spectroscopy. The data are consistent with linear dependence of frequency on pressure for the $B1$ phase of KI [Fig. 3(b)]; however, our slope of 15.2 cm^{-1}/GPa (Table II) is considerable less than the value of 18.8 previously determined at low pressure.[20–22] Because the present slope is obtained from high pressure data [Fig. 3(b)] and because KCl-$B1$ shows curvature for $\nu(P)$ as shown below, $d\nu/dP$ is inferred to decrease with pressure and that the initial slope is best constrained by previous low pressure data.[21]

IR frequencies of the $B2$ modes at the transition are substantially less (32 cm^{-1}) than those of the $B1$ phase, as previously observed,[20] in accord with the longer bonds in $B2$. The pressure dependence of the TO mode for the $B2$ phase is constrained by 11 spectra taken over 2 to 35 GPa [Table I, Fig. 3(a)]. The LO mode was observed over a narrow range, owing to interference with NaCl spectra, but it appears to parallel the behavior of the TO mode. The slope of the LO

mode (Table II) is indistinguishable from that determined through impurity induced Raman spectra,[9] but our values are 10 cm^{-1} higher. The difference in peak position is probably due to dispersion because the Raman measurement samples the edge of the Brillouin zone, whereas IR spectroscopy samples the center.

Pressure dependence of the B2 IR modes in KBr. The $B1$ phase for KBr was not observed. Previous measurements[19,21] indicate a steep (Table II) initial slope [Fig. 3(b)]. The TO mode for $B2$ phase increases nonlinearly with pressure [Table I(e), Fig. 3(a)] and is accurately represented as a quadratic polynomial in P. The frequency at the transition was not determined requiring that we use the previous measurement[20] of 115 cm^{-1}. This data point is consistent with our higher pressure trend and is bracketed by the $B2$ modes of KCl and KI (Table III). The drop in frequency of 30 cm^{-1} is close to decreases for KI and KCl. The LO mode was not detected. A slope of 7.1 cm^{-1}/GPa previously observed from impurity-induced Raman spectra of the LO mode[9] is similar to the present slope for the TO mode.

Pressure dependence of the B1 IR modes in NaF. The thin-film spectrum at 0.4 GPa has a strong peak at 253 cm^{-1} which is slightly offset from the position of the transverse optic (TO) at 244 cm^{-1} obtained from the reflectance spectrum of single-crystal NaF at ambient conditions, and a weak peak at 417 cm^{-1} which matches the longitudinal optic (LO) component (Fig. 4). Peak positions increase nonlinearly with pressure (Fig. 5). The TO mode is constrained by 12 data points which span the stability range of $B1$ [Table I(d)]. Peak positions are listed sequentially. Although strong curvature of $\nu_{TO,B1}$ with pressure is seen [Fig. 5(a)], our initial slope of 10.9 cm^{-1}/GPa lies within the uncertainty of that previously obtained below 0.62 GPa.[21] A quadratic polynomial accurately describes the dependence of frequency on pressure (Table II), and gives a first order coefficient that equals the initial slope. Other functions (exponentials and logarithms) fit the data less well.

The LO component could not be traced in all spectra mainly due to its proximity to the upper cutoff of the mylar beamsplitter. The LO data have sufficient scatter that a linear description of LO frequency vs pressure adequately describes the data at low pressure (Fig. 4). For the purpose of extrapolation, the LO-TO splitting is assumed to be independent of pressure.

Pressure dependence of the KCl modes. Peak positions of 149 and 224 cm^{-1} at 0.4 GPa for the IR modes of KCl are slightly higher, as expected, from those obtained from single-crystal reflectance at 1 atm. Distinct curvature of frequency with pressure is observed for the TO mode of B1 phase [Fig. 5(b)]. Our initial slope of 17 cm^{-1}/GPa is similar to previous determinations.[21–22] A quadratic polynomial accurately describes the dependence of frequency on pressure (Table II), but its first order coefficient is much less than the initial slope. This difference indicates that a larger number of very low pressure data points are needed to precisely constrain $(dv/dP)_0$ and the polynomial fit near 1 atm, and accounts for the slight discrepancy in slope for KBr between our data and previous measurements.[21] The position of the LO mode is poorly constrained due to interference with the NaF TO mode. It is clear that the LO frequency increases, but the slope is uncertain.

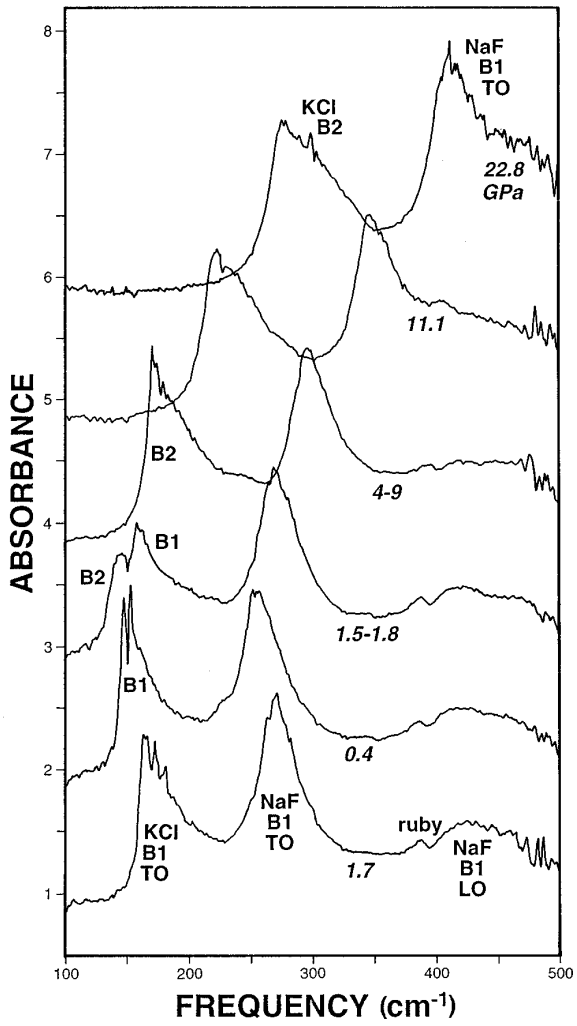

FIG. 4. Far-IR spectra of NaF and KCl at various pressures. Spectra are offset for clarity and labeled with pressures in GPa. The baseline occurs at the lowest frequencies measured and is located at about 0.2 absorbance units for each spectrum.

IR frequencies of the B2 modes at the transition are substantially less (32 cm^{-1}) than those of the B1 phase, as previously observed.[19] The pressure dependence of the TO mode for the B2 phase is constrained by nine spectra taken over 2 to 23 GPa [Table I(d), Fig. 5(a)]. The LO mode was observed to decrease similarly with pressure over the same range.

Trends in $\Delta\nu$ for the B1–B2 transition. For all halides, the drop in ν upon transformation is $\sim$20%, which is comparable to that calculated for the TO modes, but three times larger than those calculated (e.g., Hemley and Gordon[2]) for the LO modes. Frequencies for $B2$ phases of the K and Rb halides measured immediately upon transition recover the 1 atm values of their corresponding $B1$ phase (Table III). These observations allow prediction of both the LO and TO frequencies of the $B2$ phase compounds for which spectroscopic measurements were not made. For example, ν_{TO} of RbCl should be 116 ± 1 cm^{-1} at 2 GPa, and ν_{LO} will be 173 ± 1 cm^{-1}, whereas for NaF values of 350 ± 10 and 515 ± 15 cm^{-1} are expected.

LO-TO Splitting. Positions of the LO mode are not well established, owing to the weak intensity. For most samples,

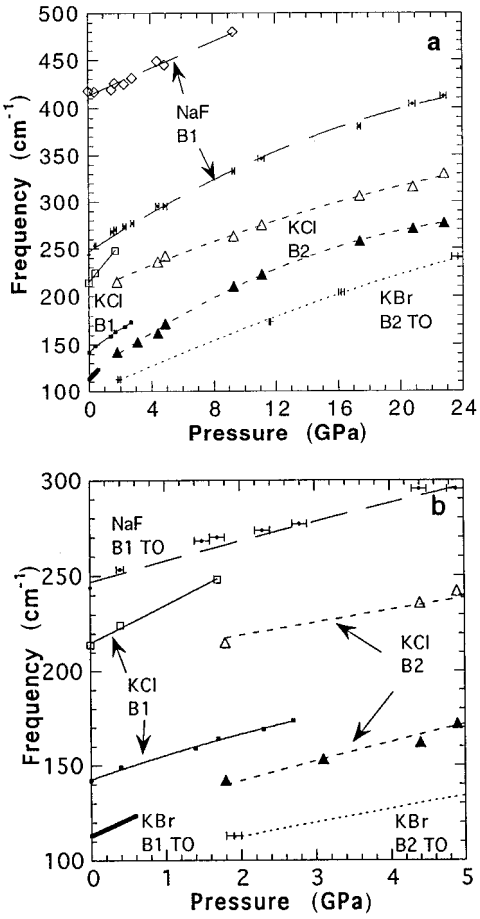

FIG. 5. Pressure dependence of IR modes. (a) High pressure data on NaF and the $B2$ phases of KBr and KCl. Small filled diamonds: TO mode of NaF in the $B1$ phase; open diamonds: LO of NaCl with the $B1$ structure; filled triangles: TO of KCl-$B2$; open triangles: LO of KCl-$B2$; small filled squares: TO of KCl-$B1$; open squares, LO of KCl-$B1$; plus sign: TO of KBr with the $B2$ structure; short thick line: data on the TO mode of KBr-$B1$ from Ref. 21. All lines are least squares fits of quadratic polynomials or linear fits in pressure to the data (Table III). (b) Low pressure expanded view.

the trend of the LO mode with pressure parallels that of the TO mode, within experimental uncertainty. For NaCl, a weak dependence of the LO-TO splitting on pressure is possible, suggesting that polarizability could change weakly with pressure. For the other samples, polarizability appears to negligibly affected by pressure, in agreement with previous determinations of peak width at low pressures.[19–22] Accurately establishing the apparently weak effect of pressure on polarizability requires further measurements of either IR absorptions at oblique angles or of the reflectance at pressure.

TABLE III. Initial and transformation frequencies.

Substance	$B1$TO at 1 atm	$B1$TO at the transition	$B2$TO at the transition
NaCl	164	391	297 [a]
KCl	142	165	142 [a] 145 [b]
KBr	113	144	115 [b]
KI	100	129	100 [a] 105 [d]
RbBr	88	96	86 [c]
RhI	75	83	72 [d]

[a]This work.
[b]Data from Postmus *et al.* (Ref. 19).
[c]From Lowndes and Rastogi (Ref. 21).
[d]Data from Ferraro *et al.* (Ref. 20).

THEORY: RELATIONSHIP OF BULK MODULI TO VIBRATIONAL SPECTRA

Blackman[17] and Brout[17] derived a semiempirical model to predict bulk modulus $K_T=-V(dP/dV)_T$ for diatomic solids from vibrational and structural data. The assumptions are (1) electrostatic attractive forces, (2) pair-wise central repulsive forces that are limited to nearest-neighbors, and (3) rigid ions. The 1 atm relation has previously been shown to agree surprisingly well with experiment[35] though zero point energies and thermal corrections were not considered. These articles[15–16,35] discuss the validity and the physical basis for the calculation of elastic properties as strain derivatives of a static crystal potential.

No additional assumptions are needed to include the effect of pressure on cubic phases.[18] The complete relation for diatomic solids at pressure is

$$K_T(P)=\frac{4P}{3}+\frac{4\pi^2\mu Q^{2/3}}{9C^2V^{1/3}}\sum_{i=1}^{3}\nu_i^2(\mathbf{k})-TV\left(\frac{\partial[\alpha K_T]}{\partial V}\right)_T+\frac{h}{2}\frac{K_T}{V}\left(\frac{\partial K_T}{\partial P}+1\right)\sum_{i=1}^{3}\left(\frac{\partial\nu_i}{\partial P}\right)_T+\frac{h}{2}\frac{K_T^2}{V}\sum_{i=1}^{3}\left(\frac{\partial^2\nu_i}{\partial P^2}\right)_T, \quad (1)$$

where μ is reduced mass, V is the molar volume, Q is the number of Bravais cells in the crystallographic cell, C is a geometrical constant relating lattice parameter to interatomic distance ($=2$ for $B1$; or $=2/\sqrt{3}$ for $B2$), α is thermal expansivity, h is Planck's constant, P is pressure, and T is temperature. The third term is the thermal correction and the fourth and fifth terms comprise the zero point correction.[36] Correction terms are needed because room temperature values are used for V and ν_i. Because $K_{\rm vib}$, the first and second terms in Eq. (1), is roughly 90% of K_T (Table IV, Refs. 37–52), the change of the correction terms with pressure should negligibly effect K_T. The independence of the sum $K_{\rm cor}$ of all four correction terms from pressure was verified for NaCl. Figure 6 shows that the experimental bulk modulus is offset by a constant from K_T calculated only from the first two terms in Eq. (1). Thus, the correction terms are obtained iteratively from Eq. (1) using only 1 atm values and the vibrational contribution as a trial values for K_T and dK/dP.

From thermodynamic identities, the thermal correction term is

$$-TV\left(\frac{\partial[\alpha K_T]}{\partial V}\right)_T=T\left(\frac{\partial K_T}{\partial T}\right)_P+T\alpha K_T\left(\frac{\partial K_T}{\partial P}\right)_T=\alpha K_T(K'-\delta_T), \quad (2)$$

TABLE IV. Vibrational, finite temperature, and zero point contributions to K_T at 1 atm.

Substance	α $1/10^6$ K	Ref.	dK_T/dT GPa/K	Ref.	K_{elastic} GPa	Ref.	Uncorrected vibrational contribution K_{vib} GPa	Finite temperature correction $T\,dK/dT$	Finite temperature correction $T\alpha K_T K'$	Optic zero point correction [b] $(hK_T/2V)(K'+1)\ \Sigma\, d\nu/dP$	Optic zero point correction [b] $hK_T{}^2/2V\ \Sigma\, d^2\nu/dP^2$	Acoustic zone boundary correction $h/2V(K'+1)\ \Sigma\,\gamma_{\text{ac}}\nu_{\text{ac}}$
LiF	97.83	37	−0.0316		67.2	41	51.43	−10.3	9.79	8.12		6.36
NaF	97.61	37	−0.0229	41, 42 [c]	46.2	27	43.04	−6.82	6.99	3.24	−0.28	1.94
NaCl	116.9	38	−0.0125	28, 43 [c]	23.56	30	20.00	−3.7	4.22	1.35	−0.33	0.76
NaBr	134.5	37	−0.0142	51	19.30	51	15.58	−4.23	4.10	1.10		0.42
NaI	137.7	37	−0.0099	49	15.01	49	10.99	−2.95	3.32	0.73		0.27
KCl	105.0	37	−0.0117	45	17.32	31	16.88	−3.48	2.93	0.80	−0.07	0.35
KBr	110.0	37	−0.0105	45, 46	14.42	32	13.95	−3.13	2.56	0.60	0	0.23(0.23) [a]
KI	117.9	37	−0.0082	47	11.49	33	10.90	−2.44	2.11	0.39	0	0.15(0.18) [a]
RbCl	114.4	39, 48	−0.010	39, 48	15.58	34	14.20	−2.98	2.91	0.67	0	0.26
RbBr	116.7	37	−0.0097	39, 42	13.02	34	12.35	−2.89	2.46	0.49	0	0.15
RbI	116.5	37	−0.0077	39, 49	10.05	34	10.00	−2.29	1.93	0.28	0	0.13
CsCl	139.5	37	−0.0147	50	16.68	50, 52	15.4	−4.38	3.94	0.56	0	0.41
CsBr	138.06	37	−0.0126	50	14.41	50, 52	13.7	−3.75	3.23	0.46	0	0.28
CsI	138.29	37	−0.0099	50	11.63	50, 52	10.6	−2.95	2.64	0.26	0	0.20

[a]Computed using $d\nu/dP$ of acoustic modes measured by Ganguly and Nicol.[9]
[b]Calculated using Table I or data in Refs. 18–22.
[c]An average of the literature values is reported.

where δ_T is the Anderson-Grüneisen parameter.[53] The thermal correction term is near zero, as evaluated in three ways: First, for alkali halides, K' occupies a narrow range of 5 to 5.6 GPa, whereas δ_T ranges from 5 to 7 (and varies as much for each substance), and the product αK_T is mostly 0.003 with LiF attaining a maximum of 0.006 GPa/K (see compilation of Ref. 54). Thus, the minimum for the thermal correction term from the representation on the right-hand side of Eq. (2) is thus -0.007 GPa and the maximum is $+0.003$ GPa. Not only is this term zero on average, but within experimental uncertainties, this term is zero for each of the alkali halides. Second, the middle representation of Eq. (2) involves more direct measurements, but this cannot be calculated accurately, regardless of whether spectroscopic or elasticity data are used, because dK/dT is uncertain. From ultrasonic and length change measurements, experimental determinations for dK_T/dT at room temperature for NaCl range from -0.0095 to -0.0158 GPa/K.[28,43] This uncertainty contributes ± 0.8 GPa to the thermal correction for NaCl. The other alkali halides have uncertainties of ± 10 to 20% for dK_T/dT. The uncertainties of the quantities in the other thermal term $T\alpha K_T K'$ are much smaller: the largest contribution stems from experimental uncertainties in K' of roughly $\pm 10\%$. Within the experimental uncertainties, the sum of the two finite temperature terms $T\alpha K_T K' + T(dK/dT)_p$ is zero (sums in Table IV range from $+0.5$ to -0.5 GPa, averaging -0.25 GPa). Third, the product αK is commonly approximated as a constant in geophysical applications. All of the above suggest that the thermal correction can be neglected.

The need for acoustic data is eliminated by taking the sums in Eq. (1) at zone center in the Brillouin zone. At zone center, the pressure derivatives of the acoustic modes might contribute to the zero point correction (ZPC) terms; however, recasting the relevant term as

$$\text{ZPC (acoustic)} = \frac{h}{2V}\left(\frac{\partial K_T}{\partial P}+1\right)\sum_{j=1}^{3}\gamma_j\nu_j,$$

where

$$\gamma_j = \frac{K}{\nu_j}\frac{\partial \nu_j}{\partial P} \tag{3}$$

indicates that this contribution is zero at zone center because the acoustic mode Grüneisen parameters γ_j are finite and small.[54] At the zone boundary, the contribution of the acoustic modes is a maximum, but even this quantity is generally small (Table IV).

The slightly negative value that is plausible for the thermal correction is apparently offset by the small positive contribution that may be possible for the acoustic zero point correction. Thus, the optical zero point correction term dominates K_{cor} and the bulk modulus is obtained[18] by modifying Eq. (1) to use only the largest (optical) zero point correction term:

$$K_T(P) = \frac{4P}{3} + \frac{4\pi^2\mu Q^{2/3}}{9C^2V^{1/3}}\sum_{i=1}^{3}\nu_i^2(\mathbf{k}) + \frac{h}{2}\frac{K_T}{V}\left(\frac{\partial K_T}{\partial P}+1\right) \times \sum_{i=1}^{6}\left(\frac{\partial \nu_i}{\partial P}\right)_T + \frac{h}{2}\frac{K_T^2}{V}\sum_{i=1}^{3}\left(\frac{\partial^2 \nu_i}{\partial P^2}\right)_T. \tag{4}$$

K_{ZPC} the third and fourth terms in Eq. (4), is calculated at 1 atm as discussed above. The second order pressure derivative

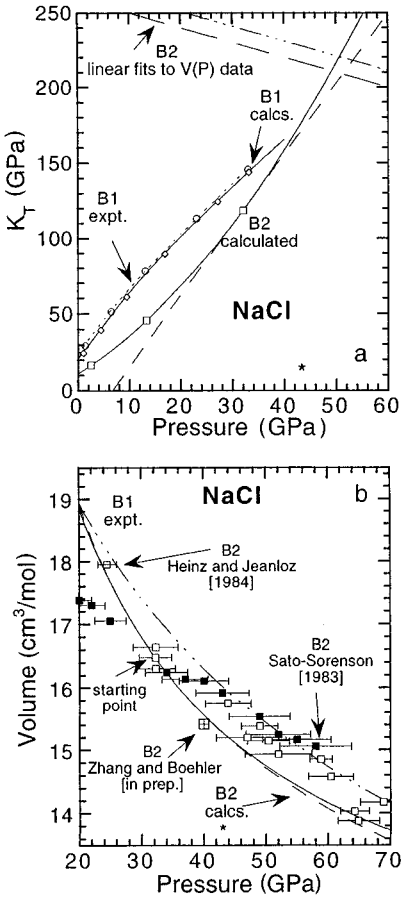

FIG. 6. Equations of state of NaCl. (a) Bulk modulus of NaCl as a function of pressure. Dotted line: compressional data for $K_T(P)$ of $B1$ phases represented by the universal EOS (Tables IV and V); solid line: $K_{\rm vib}(P)+K_{\rm ZPC}$ calculated for $B1$ using Eqs. (3) and (4) iteratively; open diamonds: $K_{\rm vib}(P)$ calculated for $B1$ using Eq. (3) but omitting $K_{\rm ZPC}$; open circles: $K_T(P)$ calculated by setting $K=K_{\rm vib}(1\ {\rm atm})+K_{\rm ZPC}+X$ equal to the ultrasonic value at 1 atm; solid line with open squares: $K_T(P)$ of $B2$ obtained from a modified Murnaghan EOS (Tables IV and V) using $K_x=K_{\rm vib}+K_{\rm ZPC}$ and K' calculated at the transition point $x=32$ GPa and for $V_x=16.5$ cm^3/mol (Refs. 5, 6, and 11); dot-dashed and short-dashed lines: K_T derived from linear fits to compression measurements on $V(P)$ for the $B2$ phase of NaCl. The asterisk marks the upper limit of the spectroscopic measurements. (b) Pressure-volume data for NaCl. Dot-dashed line, experimental $V(P)$ for $B1$ represented by the universal EOS (Tables IV and V); solid squares: data on $B2$ from Ref. 5; open squares, data on $B2$ from Ref. 6; solid line, $B2$ volume calculated iteratively from $K_{\rm vib}+K_{\rm ZPC}$ through Eqs. (3) and (4) by using $V=16.5$ cm^3/mol at 32 GPa as the ''starting point'' [this volume lies in a cluster of data points (Refs. 5, 6, and 11) as indicated]; light long-dashed line: $V(P)$ of $B2$ obtained from a modified Murnaghan EOS (Tables IV and V) using $K=K_{\rm vib}+K_{\rm ZPC}$ and K' calculated at the transition point. Square with plus sign, hydrostatic data on $B2$ by Zhang and Boehler (Ref. 65). The asterisk marks the upper limit of the spectroscopic measurements.

of the frequencies determined for a few of the alkali halides show that the magnitude of the fourth term in Eq. (4) is small and generally similar to the sum of the uncertainties (which are mainly derived from uncertainties in K').

The strong dependence of bulk modulus on spectroscopic data (as ν^2) but weak dependence on volume (as $V^{1/3}$) or bond length, allows $K_T(P)$ to be calculated independently of the equation of state through iteration. [Note: K_T is actually high order in volume, but in Eqs. (1) or (4) most of the volume dependence of K_T is contained in the vibrational frequencies.] Only the variable $\nu(P)$ and one volume at one pressure are needed. Obviously, for $B1$ phases, V_0 is used. A spectroscopic trial function for $K_T(P)$ is obtained by substituting only $\nu_i(P)$ and one volume for one specific pressure into the first and second terms of Eq. (4); the pressure independent correction term $K_{\rm cor}$ discussed above is added to $K_{\rm vib}(P)$ and this result is integrated using

$$V(P)=V_0\ \exp\left\{-\int_0^P \frac{dp}{K_{\rm vib}(P)+K_{\rm ZPC}}\right\} \qquad (5)$$

to give $V(P)$, which is then substituted into Eq. (4) with $\nu_i(P)$ to redetermine $K_{\rm vib}(P)$; these steps are repeated until iteration no longer changes $V(P)$ or $K_T(P)=K_{\rm vib}(P)+K_{\rm ZPC}$. Convergence is rapid, usually 3 or 4 iterations are sufficient. This method is advantageous in that precise determination of the initial derivative of frequency with pressure are not necessary, an EOS need not be chosen, and thus d^2K/dP^2 is a variable rather than being specified by the particular EOS (Table V, Refs. 55–57, and references therein).

For the purpose of comparison with existing ultrasonic and compression data, the results of the numerical iterations $K(P)$ were fit to various EOS (Table V). Although the equations of state developed by Holzapfel[57] are preferred because these extrapolate accurately to high pressure, his formulations were not used for the following reasons: (1) Even the lowest order of these EOS's do not yield tractable forms for $K(P)$, (2) the forms are not conducive to examining the $B2$ phases (V_0 is needed), (3) the ranges in pressure of most $B1$ phases are limited due to the phase transformation and thus K_0' is the highest order derivative needed to describe the data,[58] and (4) given the experimental uncertainties, even the relatively large range of pressure for the $B1$ phases of the sodium halides is not sufficient to allow distinction between the various EOS's. Fits to commonly used formulations such as the universal and Birch-Murnaghan EOS (Table V), were not satisfactory. Therefore, a polynomial representation for $K(P)$ calculated from spectroscopy is used for comparison (Table VI). This approach not only gave the best fit, but is commonly used in ultrasonic studies, e.g., Refs. 31–34, 52, gives K (and V by integration) that can be extrapolated beyond the range of measurements, in contrast to polynomial fits to $V(P)$ which extrapolate poorly, e.g., Ref. 3.

The above method is amenable to the $B2$ phases, for which 1 atm values are unknown (and may be indeterminate, see discussion). K_T is calculated from the $B2$ volume at transition and from the vibrational frequencies. For the $B2$ phases, $K_{\rm ZPC}$ is constrained at the transition pressure, and its uncertainty is obtained from correlations of $K_{\rm ZPC}$ for the $B1$ phases with physical parameters.

An alternate method was needed for phases for which $d^2\nu/dP^2$ was not resolved in the IR measurements. For these cases, $K(P)$ is correctly predicted near the starting pressure, but at larger pressures, $K(P)$ is overestimated from Eq. (1) or (4) because $d^2\nu/dP^2$ is always negative, not zero. Therefore, we use K_x and K_x' at the starting pressure x in a Mur-

TABLE V. Equations of state.

Name	Reference	Formulation
Universal	Vinet *et al.* (Ref. 55)	$P=3K_{T_0}\left(\frac{V_0}{V}\right)^{2/3}\left[1-\left(\frac{V}{V_0}\right)^{1/3}\right]\exp\left\{\frac{3}{2}(K_0'-1)\left[1-\left(\frac{V}{V_0}\right)^{1/3}\right]\right\},$ $K_T(P)=K_{T_0}\left(\frac{V_0}{V}\right)^{2/3}\left[2+\left\{\frac{3}{2}K_0'-\frac{1}{2}\right\}\left(\frac{V}{V_0}\right)^{1/3}-\left\{\frac{3}{2}K_0'-\frac{3}{2}\right\}\right.$ $\left.\times\left(\frac{V}{V_0}\right)^{2/3}\exp\left\{\frac{3}{2}(K_0'-1)\left[1-\left(\frac{V}{V_0}\right)^{1/3}\right]\right\}\right.,$ $K_0K_0''=-\frac{1}{4}(K_0')^2-\frac{1}{2}K_0'+\frac{19}{36}.$
Murnaghan	Birch (Ref. 56)	$V=V_0\left[1+\frac{K_a'P}{K_0}\right]^{-1/K_0'},$ $K_T(P)=K_0+K_0'P.$
Birch-Murnaghan	Birch (Ref. 56)	$P=\frac{3}{2}K_0\left[\left(\frac{V_0}{V}\right)^{2/3}-1\right]\left(\frac{V_0}{V}\right)^{5/3}\left\{1+\frac{3}{4}(K_0'-4)\left[\left(\frac{V_0}{V}\right)^{2/3}-1\right]\right\},$ $K_T(p)=K_0\left(\frac{V_0}{V}\right)^{5/3}\left\{1+\frac{1}{2}(3K_0'-5)\left[\left(\frac{V_0}{V}\right)^{2/3}-1\right]\right.$ $\left.+\frac{1}{8}(27K_0'-108)\left[\left(\frac{V_0}{V}\right)^{2/3}-1\right]^2\right\},$ $K_0K_0''=-(K_0')^2+7K_0'-\frac{143}{9}.$
Modified Murnaghan	Birch (Ref. 56); see text	$V=V_X\left[1+\frac{K_X'(P-X)}{K_X}\right]^{-1/K_X'},$ $K_T(P)=K_X+K_0'(P-X).$
HO2	Holzapfel (Ref. 57)	$P=3K_0\left(\frac{V_0}{V}\right)^{5/3}\left[1-\left(\frac{V}{V_0}\right)^{1/3}\right]\exp\left\{\frac{3}{2}(K_0'+3)\left[1-\left(\frac{V}{V_0}\right)^{1/3}\right]\right\}.$
Polynomial	This work	$K_T(P)=K_0+K_0'P+K_0''P^2.$

naghan equation of state (Table V) for $B1$ phases of KI and Rb halides and the $B2$ phases of NaCl, RbBr, and RbI. This approach is reasonable because $\sim 95\%$ of the magnitude of K_x' arises from terms involving $d\nu/dP$ as seen by differentiating Eq. (1) and by calculating K_x' with and without higher order pressure derivatives of the frequencies. For case of the $B1$ phases with $x=0$, the contribution from terms involving $d\nu/dP$ is even higher.

The calculations are compared with the best available data (see compilation of Sumino and Anderson[54]). Recent ultrasonic data, if available, were sought as this method is highly accurate. For some cases, discrepancies occur and it is not clear which study is the more reliable. For these instances average values are used in the comparison and both references are cited.

CALCULATIONS

K_T at 1 atm: *Vibrational contribution*. As expected, $K_{\rm vib}$ (Table IV) is always less than the ultrasonic determinations of K_T (Refs. 27–34, 41, 49–52). The absolute difference correlates roughly with the type of cation: $K_{\rm elastic}$-$K_{\rm vib}=11\pm 4$ GPa for Li; $=3.5\pm 0.5$ for Na; $=0.5\pm 0.2$ for K; $=0.65\pm 0.6$ for Rb; and $=1.0+0.3$ for the Cs halides (excluding KF and RbF, which differ because their cations are larger than their anion; see below). Correlations of the absolute difference with several physical properties, e.g., polarizability, bond length, and cation mass were sought using data in Refs. 54 and 59, but were found to be weak, such that separate trends exist for each of the different cations. However, the fractional difference is related to the ratio of the ionic radii r_c/r_a [Fig. 7(a)], such that a minimum occurs near $r_c/r_a=0.8$. The fractional difference similarly depends on (r_c+r_a)/bond length. In both representations, the $B1$ and $B2$ structures behave similarly. For the majority of the phases, $K_{\rm vib}$ is $94\pm 2\%$ of K_T. The Li halides are poorly described by the theory, whereas the closest correspondence is found for the potassium halides. The relationship of Fig. 7(a) can be rationalized in terms of packing in the structure. For example, rigid anions of $B1$ phases touch if $r_c<0.41r_a$, thus, for the Li halides the vibrational modes are essentially rattling of small balls in a cage, instead of breathing so that the vibrations only moderately contribute to K_T. For relatively small cations (Li and Na, except for NaF), the interactions and properties of the anions dominate the compressibility. Nearly equal size ions (NaF and the K, Rb, and Cs series excluding F) contribute subequally during compression of the solid, allowing accurate description of bulk modulus from the vibrational energies. The minimum (where the shift from ''small'' cations to subequal ionic size to

TABLE VI. Comparison of measured to calculated bulk moduli of alkali halides in the $B1$ structure (the last digits are ± 1 unless indicated differently).

		Ultrasonic study [a]						Spectroscopic EOS [c]			
Substance	V_0 cm^3/mol	K_{T_0} GPa	K_0'	K_0'' GPa^{-1}	Range GPa	Ref.	Compression [b] K_0'	K_0 GPa	K_0'	K_0'' GPa^{-1}	Range of Validity GPa
NaF	14.975	46.20	5.2	0	0–0.75	27	4.64	46.0 [e]	4.59	−0.0339(2)	0–40
NaCl	26.985	23.8 [d]	5.10 [d]	−0.37 [d]	0–32 [d]	28,29	4.82	20.0 [f]	4.45	−0.0215(2)	0–40
		23.56	5.11(3)	−0.0034(14)	0–1	30		21.0 [e]	4.45	−0.0221(2)	0–40
								≡23.56 [g]	4.45	−0.0224(2)	0–40
KCl	37.529	17.32	5.41	0	0–0.33	31	4.93	17.60(8) [e]	4.94	−0.088	0–6
								≡17.3 [g]	4.99	−0.076	0–5
KBr	43.272	14.42	5.42	0	0–0.5	32	5.33	14.55(6) [e]	5.22	−0.098(2)	0–7
KI	53.109	11.49	5.23(7)	−0.53(15)	0–0.3	33	5.58	11.29(4) [e]	4.84	0 [h]	0–5
RbCl	43.614	15.58(2)	5.48(7)	−0.58(21)	0–0.45	34	5.29	14.80(5) [e]	4.94	0 [h]	0–1
								≡15.58 [g]	4.92	0 [h]	0–1
RbBr	49.232	13.02(2)	5.43(7)	−0.75(25)	0–0.37	34	5.57	12.84 [e]	5.53	0 [h]	0–1
RbI	60.12	10.05	5.52(7)	−0.37(27)	0–0.30	34	5.76	10.28(3) [e]	5.08	0 [h]	0–1

[a] K and its pressure derivatives were derived from polynomial or linear fits to ultrasonic data and do not include $V(P)$, except for NaCl.
[b] Compression data (Ref. 69) to 40 Gpa were fit to Holzapfel's (Ref. 57) EOS (H11) using K_0 constrained by ultrasonic data.
[c] Polynomial fits were derived using V_0 and the spectroscopic data iteratively via Eqs. (4) and (5); see text.
[d] Compression, ultrasonic and length-change data were fit to a universal EOS (see text and Table V). K'' is fixed by the format of the EOS.
[e] $K_0 = K_{\text{vib}} + K_{\text{ZPC}}$.
[f] $K_0 = K_{\text{vib}}$.
[g] K_0 is constrained to match the ultrasonic result to test whether K_0' and K_0'' values are robust.
[h] K'' was set to 0 and a Murnaghan EOS (Table V) was used because curvature of frequency with pressure was not observed, and initial slopes are reported for K_0'.

''large'' cations occurs) exists at larger r_c/r_a for the $B2$ structure because the rigid anions of $B2$ phases touch at a larger radius ration $r_c < 0.73 r_a$. The increase of the discrepancy at high r_c/r_a (RbF and KF) occurs because of increased interactions between the relatively large cations.

The relationship of Fig. 7(a) and the dependence of K_{vib}-K_{elastic} on the cation are consistent with the dependence of a number of physical properties of alkali halides on related relative ionic sizes[60] and the strong effect the cation has on physical properties such as transition pressure. These correlations will be used to constrain the correction term for the $B2$ phases.

Correction terms. The zero point correction term is roughly equal to, but generally smaller than, the discrepancy between K_{vib} and K_{elastic}. Table IV gives details for the subset of alkali halides with IR measurements at pressure. The discrepancies are largest for Na and Li, but apparently also related to the size of anion [Fig. 7(b)]. The relationship of $K_{\text{vib}} + K_{\text{ZPC}}$ to K_{elastic} is best described in terms of packing, and differs little from the relationship of K_{vib} with K_{elastic}. An additional correction term is needed. The polarizability is apparently not the source of the discrepancy because the dependence of difference between predicted and measured bulk modulus on polarizability [Fig. 7(c)] is less regular than the geometrical relationships [Figs. 7(a) and 7(b)]. The geometrical correlations, in particular the increased discrepancy for small cations, suggest that the assumed form for repulsive potentials is the shortcoming of the theory (see discussion section).

Equations of state for the B1 phases. The pressure derivatives of the bulk modulus are calculated with two methods. First, only the vibrational and zero point correction terms [Eq. (4)] are used in order to establish the accuracy of the calculation based solely on vibrational measurements. Second, the 1 atm bulk moduli of NaCl, KCl, and RbCl are modified to match experiment in order to determine the accuracy with which K' and K'' are predicted from spectroscopy. For relative large cations (NaF, KBr, KI, RbBr, and RbI), the second method was not used because K_0 is accurately (± 0.23 GPa) predicted from $K_{\text{vib}} + K_{\text{ZPC}}$. Existing data for equations of state are determined mostly at low pressures (< 0.5 GPa). Only for NaCl, are the determinations well constrained at high pressures by various techniques and by hydrostatic methods. Most compression measurements are nonhydrostatic.

NaF with B1 structure. The iterative calculation uses V_0 from Table IV, $\nu_{\text{TO}}(P)$ from Table II, and assumes that the $d^2\nu_{\text{LO}}/dP^2$ is about half the size of the equivalent term for ν_{TO}. (Doubling this derivative or setting it to zero has little effect on the results: the uncertainty reported for the calculation is derived from the latitude in described the LO mode.) The results of Eqs. (4) and (5) are compatible with all existing data [Table VI, Fig. 8(a)], within experimental uncertainties.

The spectroscopic determination of volume is compatible with existing compression measurements over the entire stability range of $B1$ [up to 32 GPa, Fig. 8(a)], even though the spectroscopic measurements end at 22 GPa. Compression data of Vayida and Kennedy[3] is represented by a polynomial which is valid only at low pressure (their data points were

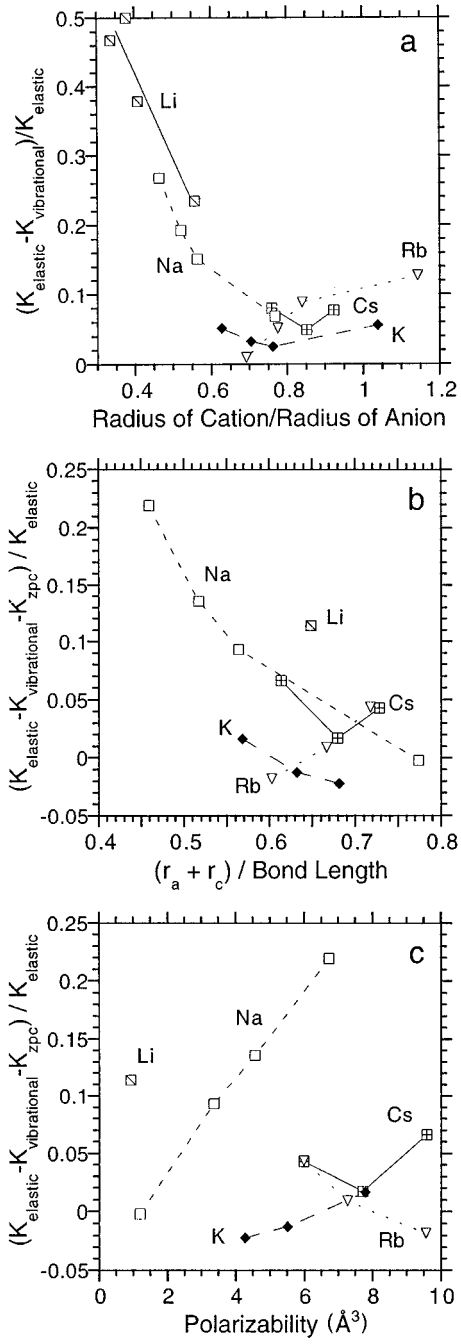

FIG. 7. Relationships of calculated and experimental bulk modulus with physical properties. (a) Dependence of the fractional difference between the vibrational contribution to bulk modulus $K_{\rm vib}$ and the elastic measurement $K_{\rm elastic}$ on the ionic radius ratio. Symbols indicate the various cations. The trend for the $B2$ structure (Cs halides) is shifted to slightly higher r_c/r_a. A strong correlation of anion properties with bulk modulus is indicated by the steep trends for Na (squares) and Li (slashed squares) halides. (b) Dependence of the fractional difference between the vibrational and zero point contributions ($K_{\rm vib}+K_{\rm ZPC}$) and the ultrasonic measurements $K_{\rm elastic}$ on the ratio of the sum of the ionic radii to the bond length. (c) Dependence of the fractional difference between the vibrational and zero point contributions ($K_{\rm vib}+K_{\rm ZPC}$) and the ultrasonic measurements $K_{\rm elastic}$ on the polarizability. Polarizability values are at $\lambda = 644$ Å (Ref. 59). Correlations exist for each of the different cations.

not reported): at low pressures, their polynomial and the present spectroscopic determination agree.

The calculated value of $K_T(0)$ matches ultrasonic measurements at 1 atm:[27] no correction terms other than the zero point contribution are need for this substance, consistent with the subequal size of the anion and cation. The calculated bulk modulus [Fig. 8(a)] curves significantly with pressure and is well described by a second order polynomial (Table VI). Our value for dK/dP of 4.17 (Table VI) is significantly less than that of 5.2 obtained in ultrasonic studies[27] but the curves are nearly indistinguishable at low pressures over which the elastic data were obtained [Fig. 8(a)]. Thus, the main difference is the present observation of curvature in K_T with pressure. Fitting the spectroscopic data to a universal EOS gives $K_0 = 42.85$ GPa and $K_0' = 4.635$; alternatively, if K_0 is constrained to be 46 GPa, then the universal EOS gives $K_0' = 4.18$ [shown as a dashed line in Fig. 8(a)]. A similarly low value of 4.34 for K' was also obtained taking the instantaneous derivative. Fitting Sato-Sorenson's[5] data to fit a universal EOS is also consistent with a low K' value. The above analysis suggests that K' reported by ultrasonic studies is too large. Possibly, nonzero values of K_0'' may hinder accurate determination of K_0' from ultrasonic data collected over a narrow pressure range.

NaCl-B1. The compression and ultrasonic data sets for NaCl-$B1$ are the most extensive and most accurate. A Universal EOS (Table IV) is used to compute volume [labeled ''expt.'' in Fig. 6(b)] and bulk modulus [Fig. 6(a)] for comparison with spectroscopic calculations. This description of volume (Table VI) is a slight improvement to the already excellent fit shown by Vinet *et al.*[55] and closely represents the available data.[61] The compressional description of bulk modulus compares well with recent ultrasonic results, except for K'' (Table VI) which is fixed by the format of the EOS (Table V).

If the vibrational contribution alone is used (the zero point correction is ignored) with frequencies that are represented as polynomials in pressure (Table II) and with the 1 atm volume as the starting point, the resulting curve lies 15% below experimental determination of K over all pressures [Fig. 6(a)]. Use of the vibrational *and* zero point terms result in a curve that lies 10% below experiment. If an additional 1 atm correction term is used such that the calculated K_0 matches the experimental determination of 23.56 GPa from recent ultrasonic data,[30] then the resulting curves for $K(P)$ and $V(P)$ are indistinguishable from those derived from compression measurements. Clearly, the effect of pressure on the zero point correction term and other correction terms is negligible. Thus, the curvature of the bulk modulus with pressure (K' and K'') can be obtained from vibrational spectroscopy, even if the match with K_0 is poor.

For NaCl, the spectroscopic calculations are well represented by a quadratic fit (Table VI). The derivatives are negligibly affected by using various correction factors. Average values are 4.45 ± 0.01 for K_0' and -0.022 ± 0.001 GPa^{-1} for K_0'. The cubic fit is marginally better, giving similar values: $K_0' = 4.59$, $K_0'' = -0.035$ GPa, and $K_0''' = 0.00025$ GPa^{-2}. If the spectroscopic calculation for $V(P)$ is fit to a universal EOS with K_0 defined as 23.56 GPa, then the derivatives are $K_0' = 5.00(1)$ and $K_0'' = -0.349(1)$, which are close to those

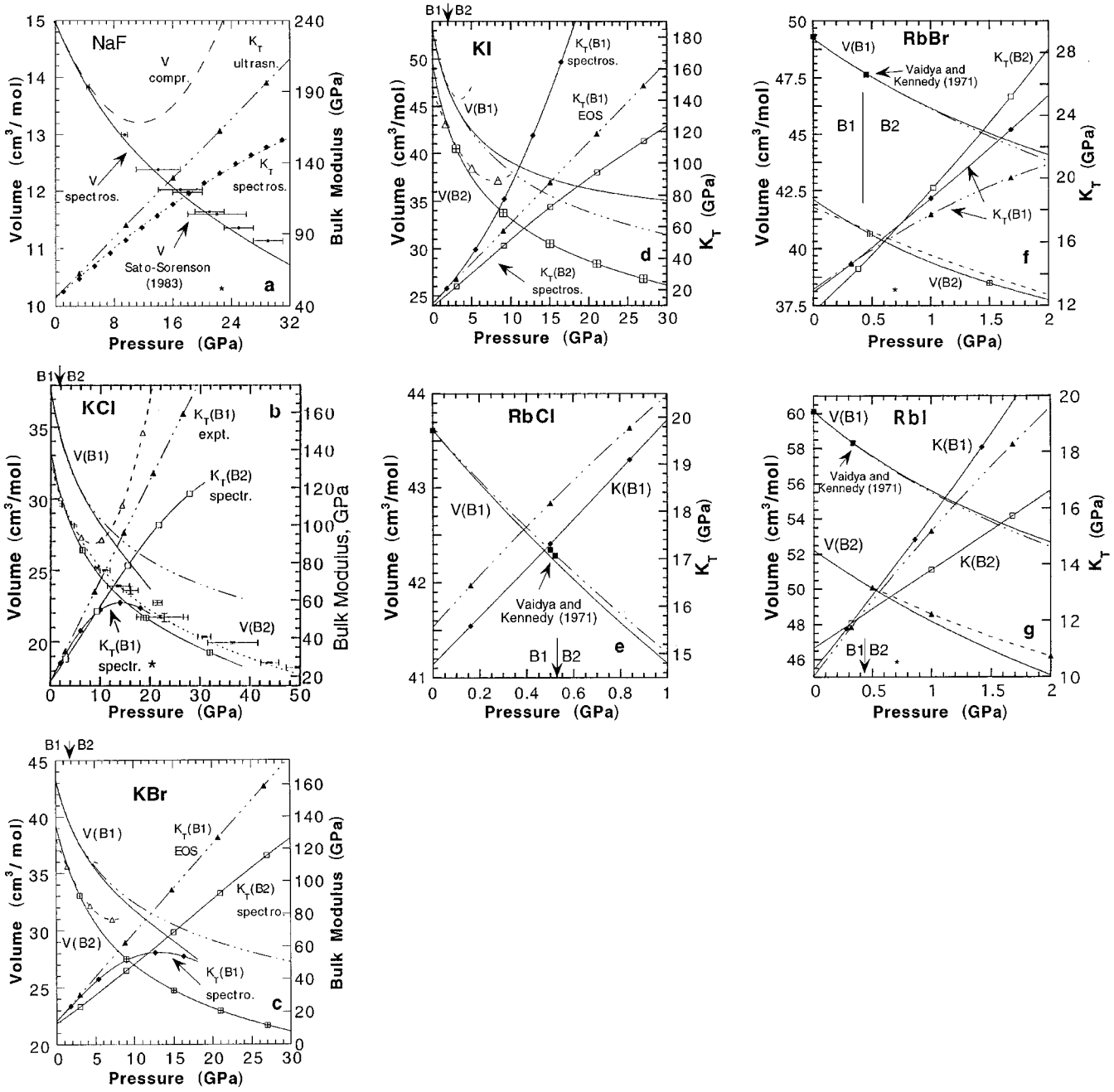

FIG. 8. Bulk modulus and volume as a function of pressure. The vertical arrow indicates the pressure at which $B1$ transforms to $B2$. The following symbols are common to most parts. Solid line: $B1$ volume calculated from spectroscopy; dashed line: $B1$ volume polynomial fit from Ref. 3; dot-dashed line: $B1$ volume calculated from ultrasonic parameters (Table IV and VI); solid line with filled diamonds: $B1$ K_T calculated from spectroscopy; dot-dashed line with filled triangles: $B1$ bulk modulus from ultrasonic parameters; solid line with square and plus sign: $B2$ volume calculated from spectroscopy; dashed line with open triangles: $B2$ volume polynomial fit from Ref. 3; solid line with open squares: $B2$ K_T calculated from spectroscopy (Table VII). The asterisk marks the upper limit of the spectroscopic measurements. (a) NaF. Small circles with error bars: $B1$ volume Ref. 5. The spectroscopic calculation for $K(P)$ is shown as filled diamonds, and the universal EOS fit to the calculation is shown as the short dashed line. (b) KCl. Crosses with error bars are $V(P)$ data from $B2$ from Campbell and Heinz (Ref. 7). Short dashed line: Murnaghan EOS calculated with K_0 and K_0' from spectroscopy, but $K_0''=0$. (c) KBr. (d) KI. (e) RbCl. (f) RbBr. (g) RbI. For (e), (f), and (g), the polynomial fits to $V(P)$ by Ref. 3 are shown as filled squares.

derived from the compression data. However, this approximation (not shown) does not fit the calculated $K_T(P)$ nearly as well. This misfit and the ultrasonic determination[30] indicate that format of the universal EOS yields results in too large a magnitude for K_0'' (the Birch-Murnaghan EOS also requires a large magnitude for K_0''). Consistent with the interdependence of K' and K'' (Table V), the initial values for K_0' derived from the universal or Birch-Murnaghan EOS are also large.

KCl-B1. The bulk modulus for KCl-$B1$ was calculated iteratively from V_0 and $\nu_i(P)$ given in Table II by assuming that the LO and TO modes are parallel. Over the narrow pressure range of 6 GPa, approximating the curvature and the position of the LO mode has little effect. The result from

Eq. (4) at low pressure [Fig. 8(b), Table VI] is similar to the Murnaghan EOS derived using ultrasonic data.[31] The difference (maximum of 4% at 2 GPa) is due to the curvature observed through spectroscopy. The calculation is valid over the $B1$ stability range and can be extended to about 6 GPa. Constraining the initial value to equal the ultrasonic result changes the pressure derivatives only slightly (Table VI).

Volumes derived from spectroscopy, ultrasonic measurements,[31] and compression studies[3] are in excellent agreement ($<0.27\%$ difference) over the stability range of $B1$ [Fig. 8(b)]. Clearly, integrating to obtain volume serves as a smoothing routine.

KBr-B1. The bulk modulus for $B1$ was calculated iteratively from V_0 (Table V) and $\nu_i(P)$ in Table II by assuming that the LO and TO modes are parallel and that the curvature of both modes is the same as that of the TO modes of KCl. The approximation [Fig. 8(c), Table V] lies close to that derived from a Murnaghan EOS using ultrasonic values. The maximum difference is 3% at 2 GPa. Volumes derived from spectroscopy, ultrasonic measurements[32] and compression studies[3] are in excellent agreement ($<0.5\%$ difference) over the stability range of $B1$ [Fig. 8(c)].

KI-B1. The bulk modulus for $B1$ calculated iteratively from $\nu_i(P)$ in Table II and from V_0 lies close to that derived from a Murnaghan EOS using ultrasonic values [Fig. 8(d)]. The maximum difference is 8% from 0 to 6 GPa. The spectroscopic K_T for $B1$ has a positive second derivative (Table VI) and behaves poorly at high pressure because a linear relation for frequency was used (the expected negative second derivative for frequency was indicated by comparison of our measurements to previous data, but could not be adequately constrained). Despite these problems, volumes derived from spectroscopy, ultrasonic measurements,[33] and compression studies[3] are in excellent agreement ($<1\%$ difference) over the stability range of $B1$ [Fig. 8(d)]. Use of the initial spectroscopic determination of 4.84 for K_0' in a universal or Murnaghan EOS (not shown) results in a better fit to $V(P)$ and is a good match to the ultrasonic data at low pressure.

RbCl-B1. Spectroscopic data are only available for the $B1$ phase.[21] The bulk modulus for $B1$ calculated iteratively from this data and by assuming that the LO-TO splitting is constant, lies 0.6 GPa below that derived from a Murnaghan EOS using ultrasonic values[34] over the stability range [Fig. 8(e)]. Requiring the spectroscopic calculation to match the ultrasonic derivation of K_0 has little effect on the slope K_0', but improves the fit with volume to better than 0.2% (not shown). The value for K_0' of 4.92 from spectroscopy may be lower than the ultrasonic determination of 5.5 because these data were fit to a quadratic with a large negative K_0'' value, but the difference could also result from the external pressure calibration used in the spectroscopic measurements.[21] The very large K_0'' value from ultrasonic data is not consistent with $d^2\nu/dP^2$ being close to zero.

RbBr-B1. The TO mode of the $B1$ phase linearly increases with pressure.[21] The bulk modulus for $B1$ calculated iteratively from this data and by assuming that the LO-TO splitting is constant (Table VI), lies close to that derived from ultrasonic values[34] for K_T and K_0' [Fig. 8(f)]. The maximum difference is 1.4% over the stability range of $B1$. Calculated volume is in excellent agreement with experiment [Fig. 8(f)].

RbI-B1. Calculations of the $B1$ volume and K_T from previous spectroscopic data[21] are in good agreement with experiment [Fig. 8(f) and Table VI].

Equations of state for high-pressure B2 phases. In general, previous determinations of the $B2$ phases, whether by compression or ultrasonic techniques, are less accurate than those of the $B1$ phases, largely due to the increased nonhydrostaticity at high pressures and to the hysteresis of the transition. Our aim is thus to calculate the $B2$ properties as accurately as possible, using the comparison with $B1$ phases as a guideline. For the iterative calculations, the volume at the transition V_x is used as the starting point, because the amount of shear stress should be negligible immediately after $B2$ is formed due to loss of volume upon recrystallization. K_{ZPC} is also calculated at the transition pressure [Eq. (4)]. For the K and Rb halides which transform at low pressures, this quantity is small and differs little from K_{ZPC}, at 1 atm. For NaCl, the high transition pressure may result in K_{ZPC} differing from the 1 atm value, and an additional correction factor may be needed as was the case for $B1$. These possibilities are considered and a detailed analysis is given for NaCl.

Problems with previous data on K_T and $V(P)$ for NaCl-B2. Compression data with which to compare our results are problematic. The recent static compression data sets[5–6] for the $B2$ phase of NaCl are compatible, differing only below 30 GPa (Fig. 6) where $B2$ is metastable. The sole measurement below 30 GPa of Heinz and Jeanloz[6] lies on the $V(P)$ curve for $B1$ (within experimental uncertainty). Because high pressure diffractions are only collected over a small solid angle so that few lines are observed, a reversion to $B1$ may have been overlooked. In contrast, Sato-Sorensen's[5] $V(P)$ data for $B2$ below 30 GPa could not have been misidentified because each of these experiments contains diffraction lines from both phases in each experiment. However, the $B2$ diffractions could have originated in the high pressure area of the cell, so that the reported average pressure is not necessarily appropriate. Moreover, partially transformed samples have been shown to give structural parameters which are not always accurate.[62]

It is significant that virtually all $V(P)$ data for $B2$ at pressures above 40 GPa lie within the uncertainty of the $B1$ curve [Fig. 6(b)]. The strong shear stress present at high pressure in such nonhydrostatic experiments can produce overly large lattice parameters and anomalously high determinations of bulk moduli.[15] Moreover, none of the accepted equations of state (e.g., the universal EOS or finite strain) adequately describes the $V(P)$ data for $B2$. The best description is a straight line:

$$V_{B2} = 18.752 - 0.06919P, \tag{6}$$

excluding the suspect datum at 25 GPa, or

$$V_{B2} = 18.953 - 0.07288P, \tag{7}$$

if all data are included. The linear appearance of $V(P)$, see Fig. 6(b), and sometimes ''reverse curvatures'' have been

TABLE VII. Spectroscopic determination of bulk moduli of alkali halides with the $B2$ structure.

Substance	Transition GPa	V_x [a] cm^3/mol	$K_{ZPC}(x)$ GPa	$K_x = K_{vib} + K_{ZPC}$ GPa	K_0 GPa	K_0'	K_0'' GPa^{-1}	V_0 cm^3/mol	EOS	Range GPa
NaF	30	10.0 [b]	~6	146(5) [c]						
NaCl	32	16.5 [d]	5.7	119(4) [g]	indeterminant	4.7(7)	≡0 [h]	indeterminant	Modified Murnaghan	20–50 [e]
KCl	1.9	30.323 [f]	0.25	24.45	17.28	4.38	−0.0283(4)	33.248	Polynomial	0–30
KBr	1.9	34.782 [f]	0.45	19.87	11.16(9)	4.33	−0.0060(2)	39.034	Polynomial	0–40
KI	1.9	42.858 [f]	0.5	17.24	9.87(11)	4.450(14)	−0.016	49.585	Polynomial	0–35
RbCl	0.5	35.483 [f]	est. 0.7	19.3 [c]						
RbBr	0.45	40.703 [f]	0.8	15.36	11.48	7.53	≡0 [h]	42.13	Modified Murnaghan	0–1
RbI	0.5	50.09 [f]	0.1	12.43	11.05	2.77	≡0 [h]	52.271	Modified Murnaghan	0–1

[a]Derived from compressional measurements of volume at the transition point as pressure was increased.
[b]From Sato-Sorensen (Ref. 5).
[c]Derived from trends in frequency across the transition.
[d]From Refs. 5, 6, and 11.
[e]V of NaCl in the $B2$ phase can be approximated at 4.4% less than $V(B1)$ at pressures above 40 GPa.
[f]Data from Vaidya and Kennedy (Ref. 3).
[g]See text for discussion.
[h]For constant $d\nu/dP$, K_0' is assumed constant and is determined at the transition pressure.

observed for various samples under shear stress (see comparisons of hydrostatic and nonhydrostatic data in Refs. 15 and 63).

Derivation of K_T from existing compression data for $B2$ is thus problematic. However, at the midpoint of the data (50 GPa), the linear fit could give a correct bulk modulus, if the compressibility data at the endpoints of the nonhydrostatic measurements lie on the true $V(P)$ curve, as has previously been observed.[15,63]

Calculation of the bulk modulus of NaCl-B2 at the transition. V_x of 16.5 cm^3/mol at 32 GPa is indicated by several studies.[5–6,11,64] Substituting frequency as a function of pressure (Table II) and this particular volume into Eqs. (4) and (5) and iterating gives K_T as 118.6 GPa at 32 GPa. The difficulty in accurately determining the LO mode contributes an uncertainty of ± 1.5 GPa. K_{ZPC} of 5.7 GPa (Table VII) may be overestimated because the calculation is done at 32 GPa instead of 1 atm. For comparison, K_{ZPC} of the $B1$ phase at 1 atm is 1 GPa, but an additional correction of 2.6 GPa is needed (see above sections). Considering these problems, the bulk modulus of $B2$ could range from 113 to 124 GPa. A decrease in K_T across the transition is clearly indicated because the drop of 23 GPa is at least four times the uncertainties in the calculation. The decrease across the transition clearly stems from the large drop in the IR frequencies and can be visualized as the release of tension in the interatomic ''springs''(see discussion section).

Pressure dependence of the bulk modulus and volume for B2. At the 32 GPa transition, the spectroscopic calculation yields K' of 4.7 ± 0.7 for $B2$. Because K' cannot be determined without knowledge of $d^2\nu/dP^2$, we assume K' is a constant. The resultant linear extrapolation of the spectroscopic results for $K_T(P)$ and use of a modified Murnaghan equation (Table V) for V (Fig. 6) constitute upper limits for K_T and for $V(P)$ because d^2K/dP^2 must be negative just as $d^2\nu/dP^2$ is negative. For NaCl, the bulk modulus follows a λ curve [Fig. 6(a)]: K_T rises from 1 atm to a local maximum at the stability limit of $B1$, drops upon transformation to $B2$, and then rises with pressure, passing the $B1$ values at about 40 GPa. At 50 GPa, the calculated $B2$ bulk modulus intersects the bulk moduli determined by linear fits to the compression data.[5–6] K_T obtained from the linear fits to compressional data near the midpoint agrees with our results because the linear representation represents a tangent to the $K(P)$ curve. Thus, the spectroscopic determination is compatible with the trends in the $V(P)$ data, within the respective uncertainties.

Use of a modified Murnaghan equation presents a problem at low pressure, because negative values are obtained for K_T below 7 GPa. Other EOS (such as higher-order finite strain or the universal formulation) yield similarly odd behaviors, as implied by their mathematical forms. Furthermore, the expected curvature of frequency with pressure would yield even more negative values of K_T at low P from Eqs. (4) and (5). These unexpected features for $K_T(P)$ are attributed to the combination of the $B1$-$B2$ transition occurring at very high pressures and to the instability of $B2$ at low pressures (discussed further below).

The uncertainty in the slope $d\nu_{LO}/dP$ (Table II) negligibly affects $V(P)$. Above 45 GPa, the volume should decrease at a faster rate than calculated (Fig. 6) because K' is not constant, but decreases with pressure. A reasonable estimate is that the $B2$ curve above 45 GPa parallels the projected $B1$ volume curve, although the $B2$ volume could decrease more rapidly than the $B1$ volume as is calculated for the potassium halides (see below).

Hydrostatic measurements of the volume for the $B2$ phase[65] are consistent with our calculation [Fig. 6(b)]. Moreover, the steeply trending data points near 32 GPa and the isolated datum on the metastable $B2$ phase of Ref. 6 near 24 GPa lie on our curve, although the latter may be a coinci-

dence as this point also lies on the $B1$ curve. Our calculation does not support the low pressure measurements of Sato-Sorensen,[5] nor does it correspond with $V(P)$ data above 40 GPa of either Sato-Sorensen[5] or of Heinz and Jeanloz[6] (which lie on the $B1$ curve, and are thus suspect). Shear stress is implied[14,15] to affect the previous measurements in that diffractions collected from the DAC involve 100 to 1000 contiguous unit cells in order to produce x rays sufficiently intense for detection and that large pressure gradients exist over this distance at the high pressures attained. In contrast, IR vibrations originate in nearest-neighbor interactions (otherwise glasses would not have spectra) so that shear stress minimally affects IR spectra (see Ref. 66, and citations therein). Shear is also reduced in our experiments due to the proximity to the volume reducing transition. Problems in the $V(P)$ measurements begin at pressures beyond our range.

KCl-B2. For $B2$, we use $\nu(P)$ of Table II in Eqs. (4) and (5) and constrain volume to match Vaidya and Kennedy's[3] measurement of 34.964 cm^3/mol at 1.8 GPa. The nonhydrostatic measurements of volume of Campbell and Heinz[7] are similar. Volumes for $B2$ derived from spectroscopy [Fig. 8(b), Table VII] lie within the uncertainty of compression up the limit of the spectroscopic data (20 GPa).

Because V_0 is unknown for the $B2$ phase, fitting the compressibility data to an equation of state yields a large variation in possible values for K_0 and K_0'. Campbell and Heinz[7] obtain $V_0 = 31.84$ cm^3/mol and $K_0 = 28.7$ GPa by assuming $K' = 4$. The data are equally compatible with $V_0 = 33.52$ cm^3/mol and $K_0 = 14.9$ GPa with $K' = 4$ and constant, and thus, the compressibility data are compatible with parameters derived from the spectroscopic calculations.

Acoustic measurements have been made of the P velocity of KCl in the $B2$ phase at nonhydrostatic pressures.[8] Obtaining the bulk modulus from this data requires estimation of the shear velocity. Acoustic measurements of KBr and KI (Ref. 9) show that the S and P velocities respond differently to the transition, so that assumptions of proportionality, as used in Ref. 8, are suspect. More importantly, the extraction of K_T from V_P requires use of an EOS and is sensitive to the assumed values for V_0 and K_0'. Given these problems, Campell and Heinz[8] do not report a bulk modulus for KCl, and thus their results cannot be compared to ours.

KBr-B2. For $B2$, we use $\nu_{TO}(P)$ of Table II and assume that the LO and TO modes are parallel. The volume at the transition (Table VII) determined from compression data was used as a constraint. The assumption of parallel slopes contributes a small error: for example, assuming that the LO-TO splitting decreases to nothing at 35 GPa only decreases K_T by 5%. A decrease in the LO-TO splitting similar to that of KCl would affect K_T by less than 1%, and the resulting uncertainty in volume is inconsequential. Volumes for $B2$ derived from spectroscopy [Fig. 8(c), Table VII] and compression measurements are similar, differing by a maximum of 2.5% at the limit of the compression measurements (4.5 GPa), but vary considerably in slope [Fig. 8(d)]. The difference can be attributed to the narrow range of pressure measurements for the compressional studies and to use of a low order polynomial to model the data.

KI-B2. For $B2$, we use $\nu_{TO}(P)$ of Table II and assume that the parallel slopes observed from 2 to 5 GPa for the LO and TO modes [Fig. 3(a)] continue to higher pressures. The assumption of parallel slopes contributes little error as discussed above. Volumes for $B2$ derived from spectroscopy [Fig. 8(d), Table VII] and compression measurements are close. The relationship is as described for KBr, above.

RbBr-B2. For $B2$, we use $\nu_{TO}(P)$ of Table II and assume that the LO-TO splitting is constant and equal to the $B1$ value. Volumes for $B2$ derived from spectroscopy [Fig. 8(f), Table VII] and compression measurements[3] agree moderately well, differing by a maximum of 2.5% at the limit of the compression measurements (4.5 GPa). K' for $B2$ (Table VII) is uncertain because the slope $d\nu/dP$ was determined over a narrow interval of 0.12 GPa at the limit of the measurements.[21]

RbI-B2 Spectroscopic data for $B2$ of Ref. 19 were used, but these may not be an accurate representation of the evolution with pressure because an ungasketted diamond-anvil cell was used. The low slope of the $B2$ mode constrains the value attained after transition, allowing accurate calculation of K_T near the transition (Table VII), but the values of K_0 and K' are suspect.

NaF-B2 and RbCl-B2. Because $\nu(P)$ data are not available, bulk moduli at the transitions (Table VII) were calculated from the predicted frequency drops. For K_{ZPC}, $d\nu/dP$ with half of the value of that for the $B1$ phase was used, as appears to be the general rule (Table II). The uncertainty in the bulk modulus for NaF is large because calculation of K_{ZPC} at high pressure is uncertain. Fitting recent compressional determinations of $V(P)$ for RbCl-$B2$ to a Murnaghan EOS gives $K_0 = 17.9(10)$ GPa and $K_0' = 5.23(29)$, assuming that V_0 is 31.45 cm^3/mol (Ref. 8). These parameters give 20.5 GPa as the bulk modulus at the transition, which is within the uncertainty of our calculation. The V_0, K_0, and K_0' parameters are highly interdependent, so that K and K' derived from compression data are more uncertain than previously stated.[7–8]

DISCUSSION AND CONCLUSIONS

Accuracy of the model: K_T at 1 atm for B1 phases. The calculated values for $K_0 = K_{vib} + K_{ZPC}$ are fairly precise, with uncertainties mainly arising from the correction term. The calculation (Tables IV and VI) is accurate within 0.5 GPa (0.4 to 5%) for all substances with a cation radius greater than 0.6 times their anion's radius. For NaCl with $r_c/r_a = 0.56$, the theory errs moderately (± 2 GPa $= 10\%$), and for relatively smaller cations, the discrepancy increases. Thus, for K, Rb, and Cs halides, the semiempirical calculation is more accurate than recent quantum mechanical (QM) approaches which generally err by 10 to 25% (Refs. 1, 2), whereas for Na halides, the accuracies are comparable, and for Li halides QM approaches are more accurate.

Pressure derivatives for the B1 phases. The EOS for the alkali halides determined from spectroscopy is represented by a polynomial in pressure (Table VI), which is then integrated to obtain $V(P)$. $K(P)$ is a rapidly converging series, because terms of order P^2 and higher are small and because the signs of polynomial coefficients of $\nu(P)$ are alternately positive and negative. A polynomial representation is given for $K_T(P)$ because this involves the least interdependence of K' and K''. The polynomial result can be extrapolated to

almost twice the pressure limit of the experiment, suggesting the reasonableness of the representation. Also, the existence of good fits of K as a quadratic in P for all the substances examined suggests that K''' is very close to zero.

The slopes K' and K'' are related to $d\nu/dp$ and $d^2\nu/dP^2$, respectively, and are negligibly affected by the uncertainty in predicting K_0. The uncertainties (Table VI) are derived from the fits to the spectroscopic calculation. Additional uncertainty could arise in K_0' due to the range of pressure and the number of data points involved in computing $\nu(P)$. Possibly, total errors could be as much as 1% for NaCl, 2% for NaF, 5% for KCl and KBr, and 10% for the others. The spectroscopic determination of K' for Rb halides is very uncertain as the pressures were obtained from external calibrations. The second derivative K'' is readily obtained if curvature of frequency with pressure is observed. The accuracy of K_0'' is roughly 5% for NaCl and 10% for the others.

Calculation of $K_T(P)$ and $V(P)$ from only V_0 and $\nu_i(P)$ appears to be accurate for the low pressure $B1$ polymorphs from comparison with ultrasonic and compression data. The ultrasonic measurements for K'' bracket our results (Table VI). For NaCl, which has the best constrained spectroscopic and elastic measurements, use of the same EOS gives the same values for K' and K'' from spectroscopy and from ultrasonic, compression and length-change data (Table VI). Thus, the difference between the spectroscopic calculations and ultrasonic or compressibility measurements is partially due to the choices in representing EOS data (Table IV, Refs. 55–57). For the other alkali halides, the determinations were made over such narrow ranges of pressure that the curvature K'' is poorly controlled. The large values (~ -0.3/GPa) of K'' from earlier ultrasonic studies are probably not correct in that recent studies[30] give much smaller values of -0.003/GPa.

Calculated K' values are consistently 0.5 GPa smaller than those derived from ultrasonic measurements, whereas the most recent compression data[69] yield small K_0' values, comparible to the present results. The difference for NaCl is due the choice of an equation of state as the Birch-Murnaghan and universal EOS require K_0'' to have a large magnitude, which forces K_0' to be larger to compensate. Similarly, ultrasonic determinations of K_0' could be too large when $|K_0''|$ is large (Table VI). Although ultrasonic precision for K is generally 1% (Jackson *et al.*[67]), K_0' may not be as accurate as stated: comparison of various data sets for NaCl (Ref. 68) suggests a 5 to 10% uncertainty in K_0' derived from ultrasonic studies. For example, highly regarded studies of Chabildas and Ruoff[29] and Spetzler *et al.*[28] give K_0' of 5.7 and 5.3, respectively. The various determinations of K_0' are equal, within this larger uncertainty.

The spectroscopic calculations suggest a compositional dependence such that K' is near 4.5 for Na halides, 4.9 for K halides, and 5.2 for Rb halides. Similarly, for K_0'', Na halides appear to have smaller magnitudes than K halides.

Equation of state and stability of the B2 phases. The spectroscopic calculations agree well with $B2$ compression data for $V(P)$ at moderate pressures where the IR data were collected. At increasingly higher pressures, the difference between $V(P)$ from compression measurements and vibrational calculations increases. The NaCl compression data are

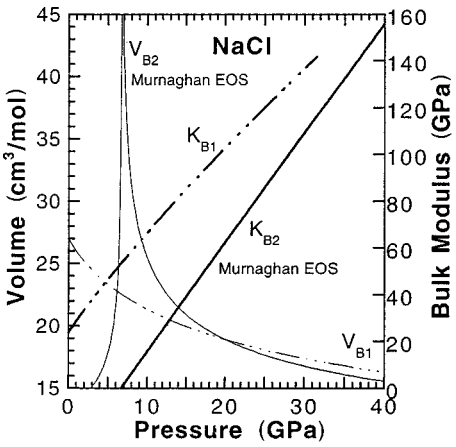

FIG. 9. Volume and bulk modulus for NaCl. Light lines: volume; heavy lines: K_T; solid line: the Murnaghan EOS based on the spectroscopic calculation for $B2$; dot-dashed lines: experimental values for $B1$.

suspect because the $B2$ volumes fall on the extension of $V(P)$ for $B1$. It is also possible that shear stress in nonhydrostatic environment for the KCl compression experiment could have affected the crystallographic results, but to a lesser extent that NaCl, because the pressures were lower.

The uncertainties in K_T of ± 4 or 5 GPa for the Na halides and of ± 0.5 GPa for K and Rb halides were estimated from the discrepancies between calculated and measured K_T for the $B1$ phases. For the $B2$ phases, ultrasonic data do not exist for comparison. Accurate determination of K_T from $V(P)$ data for $B2$ phases is difficult for several reasons. First, and most importantly, the $V(P)$ data for $B2$ begin at high pressure, so that the EOS must extract V_0 as well as K_0 and K_0' from $V(P)$. The addition of the third parameter makes determination of all three coefficients most uncertain, if not indeterminate, particularly because the $V(P)$ data show little or no curvature (Figs. 6 and 8). Second, slight errors in V lead to large variations in K_T. Third, K' of $B2$ phases is assumed to equal 4, which is lower than that of the $B1$ phases, suggesting that K_T is probably overestimated for the $B2$ phases. Fourth, use of the Murnaghan equation (Table V) to analyze $V(P)$ data which begin above ambient pressure underestimates V_0, which results in an overestimation of K_0. In particular, bulk moduli for NaCl with the $B2$ structure derived from previous compressibility measurements[5,6] are unsupported by our data, nor is it expected that such experiments with large shear stress would give correct K_T, as discussed previously.[14,15,62,63]

The calculated bulk modulus of NaCl in the $B2$ structure at 1 atm projects to zero (Fig. 9) based on the linear response of frequency to pressure, and could become negative at 1 atm as $d^2\nu_i/dP^2$ is negative when measurable for alkali halides and virtually all other solids measured. Using a Murnaghan EOS to extrapolate the spectroscopic calculation below the pressure range of our measurements yields $K_T = 0$ and infinite volume at 10 GPa. Such nonphysical behavior for K_T indicates that the $B2$ structure is unstable below ~ 10 GPa. This lower limit is not particularly sensitive to the input parameters, as similar values are attained for a wide range of K' of 5 to 7 in the Murnaghan equation. Between ~ 10 and 21 GPa, where the $B1$ and $B2$ volumes are equal, the $B2$

TABLE VIII. Percentage change[a] in properties across the $B1-B2$ transition.

Compound	$\Delta\nu_{TO}$ [a]	$\Delta\nu_{LO}$ [a]	ΔV [a]	ΔK_T Spectroscopy	ΔK_T Compression	ΔK_T Ultrasonics	ΔK_T Theory	ΔK_T Semiempirical	$\Delta K'$ [a] This work
NaF	-18 ± 3 [d]	-13 ± 3 [d]	-8 [e,i]	$-8\ \pm\ 4$ [h,i]				-5 [m]	
NaCl	-27	-16	-4.1 [e,f]	$-16\ \pm\ 3$ [f,h]			$-9\pm\ 2$ [l]	-18 [m]	$+5\pm10$ [h,i]
KCl	-16	-13	-12 [g]	$-7.5\pm\ 3$ [h,i]	$-6.8\pm\ 2.2$ [j]		$+13\pm13$ [l]	$+2$ [m]	-11 ± 10 [h,i]
KBr	-20	-15	-11 [g]	$-17\ \pm\ 5$ [h,i]	$-7.4\pm\ 0.5$ [j]			0 [m]	-17 ± 10 [h,i]
KI	-22	-20 ± 2	-10 [g]	$-19\ \pm5$ [f,h,i]	$-6.8\pm\ 1.9$ [j]			-2 [m]	-8 ± 10 [h,i]
RbCl	-7 [d]	-5 [d]	-16 [g]	$+6\ \pm8$ [f,h,d]	$-7\ \pm2$ [j]	$+17$ [k]	$+26\pm26$ [l]	$+22$ [m]	
RbBr	-10	-8 [b]	-14 [g]	$-0.3\pm\ 3$ [f,h]		$+22$ [k]		$+18$ [m]	$+38$ [f,h,c]
RbI	-13	-7 [b]	-13 [g]	$-2\ \pm\ 4$ [f,h]		$+25$ [k]		$+14$ [m]	-50 [f,h,c]

[a] $\Delta=(B2-B1)/B1$. The last digit is uncertain by ±1 or as indicated.
[b] Derived assuming the LO-TO splitting is constant.
[c] These values are estimates.
[d] Frequencies were estimated from the trends (see Table III).
[e] Volume for $B2$ from Sato-Sorensen (Ref. 5).
[f] $B1$ properties from EOS data in Table VI.
[g] Volume data from Vaidya and Kennedy (Ref. 3).
[h] $B2$ properties from the spectroscopic EOS in Table VII.
[i] $B1$ properties are from the spectroscopic EOS in Table VI.
[j] Boehler and Zha (Ref. 10).
[k] Report by Shaw (Ref. 4). The uncertainties depend on the change in length during transformation, which is unknown.
[l] The quantum mechanical calculation is from Recio *et al.* (Ref. 1). The uncertainty was estimated from the difference of the $B1$ bulk modulus from experiment. It may be larger because the $B2$ properties were calculated assuming finite 1 atm values.
[m] Figure 5 in Jeanloz (Ref. 13) was used in conjuction with recent values of ΔV and K_0' for $B1$ (Table VI). The uncertainties are large, and depend on the accuracy of K_0', and are roughly ±6 to ±10; for example, Jeanloz (Ref. 13) estimated ΔK as -12% for NaCl using 1982 data.

phase may be metastable. More likely, $B2$ metastability is limited to $P>21$ GPa, consistent with observations.[5,6,11,64]

In contrast to results for NaCl, ''normal'' behavior of V and K_T with pressure is observed for the $B2$ phases of K and Rb halides. This difference is clearly due to their low transformation pressures of 2 and 0.5 GPa, respectively. Hence, properties of the $B2$ phases of potassium or rubidium halides could be modeled by a commonly used EOS. $V(P)$ curves for the $B2$ phase of NaCl cannot be correctly modeled by existing equations of state, as those that include terms for K'' also require positive, finite bulk modulus. The Murnaghan EOS, which assumes that K' is constant, can be used, but this extrapolates poorly to very high pressures.

Changes in physical properties across the B1-B2 transformation: The sign of ΔK. Calculations based on IR measurements of alkali halides indicate that K_T generally decreases substantially across the $B1$-$B2$ transformation (Tables VI–VIII). For NaF and RbCl, K_T for $B2$ at the transition was calculated using the trends in frequency. NaF behaves similarly to NaCl. The value for RbCl (Table VIII) is similar to those derived for RbBr and RbI, however, the bulk modulus for this compound was found to slightly increase across the transition (Fig. 10) and the decreases in K_T at the transition for RbBr and RbI are much smaller than those of the other alkali halides (Tables VI and VII), lying close to zero (Table VIII).

The general decrease in K_T is corroborated by direct measurements (using a piston-cylinder apparatus) of KBr, KI, KCl, and RbCl.[10] Moreover, a strong decrease of $\sim35\%$ has been observed for the transverse acoustic frequencies (ac-

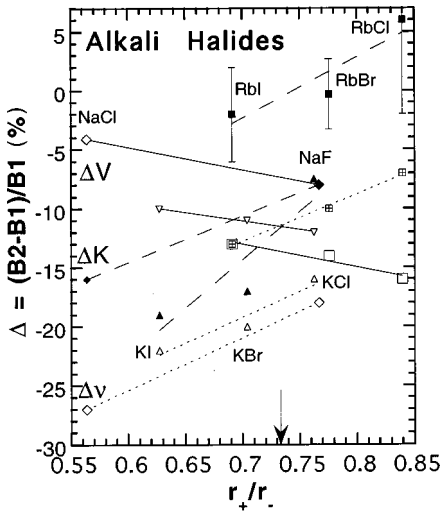

FIG. 10. Changes in physical properties across the $B1$-$B2$ transition as a function of radius ratio. Diamonds: Na halides; triangles: K halides; squares: Rb halides; dashed lines with filled symbols: differences in K_T calculated from IR measurements; solid line with open symbols: measured differences in volumes; dotted line with open symbols and crosses: measured differences in the TO frequency; heavy arrow: theoretical limit of stability for six coordination of unequal sized spheres. Sources of the data are given in Table VIII. Error bars are indicated for the change in bulk moduli for the Rb halides. Error bars are smaller for the Na and K halides.

companied with little or no change in the longitudinal acoustic modes) during transformation of KBr and KI through impurity-induced Raman spectroscopy, which is also consistent with K_T decreasing across the transition.[9] Recent QM calculations[1] support a decrease for NaCl, as do semiempirical relations of the change in K with K' values for $B1$ and with the change in volume.[13] These types of calculations are not accurate for large cations.[1]

Our results are not compatible with previous ultrasonic measurements of Rb halides (Shaw[4]) which show large increases in K_s of 15–23%. Ultrasonic determination of K_s for the $B2$ phases is problematic for several reasons. Foremost, as discussed by Shaw,[4] the ultrasonic data are affected in an indeterminate way by the change in length during transformation. In addition, the accuracy of ultrasonic measurements is not sufficient to resolve the small λ curve shown in Figs. 8(e)–8(g) owing to the sluggishness of the transition during compression, to hysteresis, and to the uncertainties in the pressure determination associated with anisotropic expansion of the salt.

K' also changes across the transformation (Table VIII). The K' data for the K halides is well constrained for the $B1$ phases from compression and spectroscopic calculations (Table VI) and for $B2$ from spectroscopy (Table VII), suggesting decrease of roughly 10%, upon transformation to $B2$.

A simple model for changes in frequency, volume, and bulk modulus across the transition. A ball and spring model of the solid corroborates our result that K_T decreases across the $B1$-$B2$ transformation. The bond strength of an ionic solid will depend roughly on interatomic distance. Because transformation to $B2$ increases the bond length, the bond strength will decrease, hence the springs are weaker and the frequency drops, as discussed previously.[70] Because there are six springs for $B1$, but eight for $B2$, the bulk modulus will decrease upon transformation for large decrease in bond strength, but could increase if the decrease in strength is offset by the larger number of springs. Thus, for Na and K halides, with large drops in ν (Table III), K_T will decrease, but for the Rb halides with small drops in ν, the change in K_T is near zero. This differs considerably from Jeanloz's conclusion[13] that ΔK depends on ΔV and that negative ΔK requires $|\Delta V| < 10\%$.

The compositional dependence of the differences in physical properties between the $B1$ and $B2$ phases ($\Delta\nu$, ΔV, ΔK_T, and $\Delta K'$) are compatible with this simple model. For each kind of cation, ΔK_T or $\Delta\nu_i$ becomes more positive the ionic radius ratio increases (Fig. 10) because relatively large cations (e.g., RbBr) push the anions apart in the $B1$ lattice, yielding bond lengths for $B1$ that are close to those occurring in $B2$, whereas the relatively small cations (e.g., NaCl) fit in the voids formed by the anions in either structure, yielding much different bond lengths in $B1$ and $B2$. In contrast, ΔV becomes more negative as the cation/anion ratio increases because the transformation removes the ''pore space'' present in the $B1$ structure due to the bigger cations forcing the anions further apart. The size and magnitude of $\Delta K'$ (Table VIII) should roughly parallel that for ΔK which is observed for the potassium halides. For the Rb halides and NaCl, the experimental determinations of K' for their $B2$ phases are uncertain.

Limitations and applicability of the semiempirical model. The semiempirical model originated by Blackman[17] and Brout[17] for calculating elastic parameters from vibrational spectra works reasonably well[18,35] because vibrational spectra essentially originate through interactions between nearest neighbors. Two of the assumptions are justified by the data: Central potentials are acceptable for such cubic structures because these scale during compression, and rigid ions are reasonable because the LO-TO splitting is roughly unaffected by pressure (Figs. 1–5) and because the polarizability is not related to the discrepancy between experiment and calculation (Fig. 7). The description of repulsive potentials as nearest-neighbor interactions appears to be the shortcoming of the model. This assumption is reasonable only for the subequal sized ions, resulting in accurate calculation for K_0, K_0', and K_0'' for this class of alkali halides. For the small cations, repulsion between the second nearest-neighbor anions is not accounted for by the theory, unless the interaction is purely electrostatic. This is probably not the case, leading to decreasing accuracy in K_0 as the cation radius decreases. Very large cations would also be a problem for the model, but only two compounds (RbF and KF) are affected and this is only to a minor extent because the difference in ionic sizes is small. The summations used in deriving Eqs. (1) or (4) could be recast to include a repulsive term between the second nearest neighbors only if that potential is proportional to the first nearest-neighbor interaction.

The spectroscopic calculation is complementary to quantum mechanical approaches. First, the semiempirical calculation provides information on K' and K'' which are not generally calculated in QM approaches. Second, the present method is amenable to large cations for which QM (Refs. 1, 2) falters, and vice versa.

ACKNOWLEDGMENTS

The IR measurements were performed at the Geophysical Laboratory. Support for this project was provided by NSF Grant No. EAR-8419984 and by the David and Lucile Packard Foundation. Support during preparation of the manuscript was provided by the Alexander von Humboldt Foundation. Special thanks are due to R. Boehler and A. Chopelas (Max Planck Institut für Chemie, Mainz) for helpful comments. The physical model of changes in K_T across the phase boundary arose from discussions with R. Boehler.

[1] J. M. Recio, A. M. Pendas, E. Francisco, M. Florez, and V. Luana, Phys. Rev. B **48**, 5891 (1993); A. M. Pendas, V. Luana, J. M. Recio, M. Florez, E. Francisco, M. A. Blanco, and L. N. Kantorovich, *ibid.* **49**, 3066 (1994); M. Prencipe, A. Zupan, R. Dovesi, E. Apra, and V. R. Saunders, *ibid.* **51**, 3391 (1995). These articles summarize earlier calculations.

[2] For example, J. L. Feldman, M. J. Mehl, and H. Krakauer, Phys. Rev. B **35**, 6395 (1987); R. J. Hemley and R. G. Gordon, J. Geophys. Res. **90**, 7803 (1985).

[3] S. N. Vaidya and G. C. Kennedy, J. Phys. Chem. Solids **32**, 951 (1971).

[4] G. H. Shaw, J. Geophys. Res. **79**, 2635 (1974).

[5] Y. Sato-Sorensen, J. Geophys. Res. **88**, 3543 (1983).

[6] D. L. Heinz and R. Jeanloz, Phys. Rev. B **30**, 6045 (1984). Note: although these authors claim a decrease of 8% in K_T for NaCl, their reported parameters of $K_0 = 36 \pm 4$ and K_0' defined as 4 give $K_T(B2) = 164$ GPa at the transition which is 15% higher than K_T of the $B1$ phase at the transition (see Refs. 55 and 61). Apparently, they did not account for nonzero K'' for $B1$.

[7] T. Yagi, J. Phys. Chem. Solids **39**, 563 (1978); H. H. Demarest, Jr., C. R. Cassell, and M. A. Dunn, *ibid.* **39**, 1211 (1978); W. A. Bassett and T. Takahashi, in *Advances in High Pressure Research 4*, edited by R. H. Wentorf, Jr. (Academic, New York, 1974), pp. 165–247; A. J. Campbell and D. L. Heinz, J. Phys. Chem. Solids **52**, 495 (1991).

[8] A. J. Campbell and D. L. Heinz, Science **257**, 66 (1992); J. Geophys. Res. **99**, 11 765 (1994). Note, only v_P is measured.

[9] B. N. Ganguly and M. Nicol, J. Appl. Phys. **47**, 2467 (1976); A. Chopelas, Earth Planet. Sci. Lett. **114**, 185 (1992); gives relations between acoustic velocities and bulk modulus.

[10] R. Boehler and C. S. Zha, Trans. Am. Geophys. Union (EOS) **68**, 1470 (1987).

[11] W. A. Bassett, T. Takahashi, H.-K. Mao, and J. S. Weaver, J. Appl. Phys. **39**, 319 (1968).

[12] This idea has its roots in velocity/density systematics [F. Birch, Geophys. J. R. Astron. Soc. **4**, 295 (1961); D. L. Anderson, *ibid.* **13**, 9 (1967)] which are largely derived from polyatomic oxides and the assumption that compression and phase changes have the same effect, despite the facts that different structures fall on different trends; that deviations are known to exist from the general trends [T. S. Shankland, J. Geophys. Res. **77**, 3750 (1972)], that alkali halides and oxides need not follow the same EOS behavior [O. L. Anderson and J. E. Nafe, J. Geophys. Res. **70**, 3951 (1965)], and that structural changes need not follow Birch's law [R. C. Lieberman and A. E. Ringwood, J. Geophys. Res. **78**, 6926 (1973)].

[13] R. Jeanloz, in *High-Pressure Research in Geophysics*, edited by S. Akimoto and M. H. Manghanini (Center for Academic Publication, Tokyo, 1982), p. 479. Note; both positive and negative changes in K_T across the transition are predicted, depending on the size of volume change and of the accepted value for K_0' of $B1$. The calculation assumes as simple interatomic potentials, temperature independence of entropy, $K'' = 0$, representation of frequencies by an average, and neglect of zero point energy and thermal corrections.

[14] J. C. Jamieson and B. Olinger, in *Accurate Characterization of the High Pressure Environment*, edited by E. C. Lloyd (National Bureau of Standards, Washington, D.C., 1971), Vol. 326, pp. 321–323; Y. Sato, in *High Pressure Research, Applications to Geophysics*, edited by M. H. Manghnani and S. Akimoto (Academic, New York, 1997), pp. 307–323.

[15] G. L. Kinsland and W. B. Bassett, Rev. Sci. Instrum. **47**, 130 (1976); D. R. Wilburn and W. B. Bassett, High Temp.-High Press. **9**, 343 (1976); Am. Mineral. **63**, 591 (1978).

[16] L. Boyer, Phys. Rev. B **23**, 3673 (1981); J. L. Feldman, M. J. Mehl, L. L. Boyer, and N. C. Chen, *ibid.* **37**, 4784 (1988).

[17] M. Blackman, Proc. R. Soc. London, Ser. A **181**, 58 (1942); R. Brout, Phys. Rev. **113**, 43 (1959).

[18] A. M. Hofmeister, J. Geophys. Res. **96**, 16 181 (1991).

[19] C. Postmus, J. R. Ferraro, and S. S. Mitra, Phys. Rev. **174**, 983 (1968).

[20] J. R. Ferraro, S. S. Mitra, and A. Quattrochi, J. Appl. Phys. **42**, 3677 (1971).

[21] R. P. Lowndes and A. Rastogi, Phys. Rev. B **14**, 3598 (1976).

[22] M. S. Shawyer and W. F. Sherman, Infrared Phys. **22**, 23 (1982).

[23] H. K. Mao and P. M. Bell, Carnegie Inst. Wash. Yrbk. **77**, 904 (1978); H. K. Mao, J. Xu, and P. M. Bell, J. Geophys. Res. **91**, 4673 (1986); H. K. Mao, C. G. Hadidiacos, P. M. Bell, and K. A. Goettel, Carnegie Inst. Wash. Yrbk. **82**, 421 (1983).

[24] A. M. Hofmeister, J. Xu, H.-K. Mao, P. M. Bell, and T. C. Hoering, Am. Mineral. **74**, 281 (1989).

[25] K. D. Moller and W. G. Rothschild, *Far-Infrared Spectroscopy* (Wiley, New York, 1970), pp. 303–324.

[26] D. W. Berreman, Phys. Rev. **130**, 2193 (1963).

[27] R. A. Miller and C. S. Smith, J. Phys. Chem. Solids **25**, 1279 (1964); W. A. Bensch, Phys. Rev. B **6**, 1504 (1972).

[28] H. Spetzler, C. G. Sammis, and R. J. O'Connell, J. Phys. Chem. Solids **33**, 1727 (1972).

[29] L. C. Chbabildas and A. L. Ruoff, J. Appl. Phys. **47**, 4182 (1976).

[30] H. S. Kim, E. K. Graham, and D. E. Voigt, Trans. Am. Geophys. Union (EOS) **70**, 1368 (1989).

[31] R. A. Bartels and D. E. Schuele, J. Phys. Chem. Solids **26**, 537 (1965); L. S. Cain, *ibid.* **37**, 1178 (1976).

[32] P. J. Reddy and A. L. Ruoff, in *Physics of Solids at High Pressures*, edited by C. T. Tomizuka and R. M. Emrick (Academic, New York, 1965), pp. 510–525.

[33] G. R. Barsch and H. E. Shull, Phys. Status Solidi **43**, 637 (1971).

[34] Z. P. Chang and G. R. Barsch, J. Phys. Chem. Solids **32**, 27 (1971).

[35] H. B. Rosenstock, Phys. Rev. **129**, 1959 (1963); S. S. Mitra and R. Marshal, J. Chem. Phys. **41**, 3158 (1964).

[36] D. C. Wallace, *Thermodynamics of Crystals* (Wiley, New York, 1972).

[37] K. K. Srivastava and H. D. Merchant, J. Phys. Chem. Solids **34**, 2069 (1973).

[38] R. K. Kirby, J. Res. Natl. Bur. Stand. Sect. A **17**, 363 (1967).

[39] M. Ghafelehbashi, D. P. Dandekar, and A. L. Ruoff, J. Appl. Phys. **41**, 652 (1970).

[40] S. Hart, J. Phys. D **10**, L261 (1977).

[41] L. E. A. Jones, Phys. Earth Planet. Inter. **13**, 105 (1976).

[42] J. T. Lewis, A. Leboczky, and C. V. Briscoe, Phys. Rev. **161**, 877 (1970).

[43] V. E. Avericheva, A. A. Botaki, G. A. Dvornikov, and A. V. Sharko, Sov. Phys. J. **16**, 583 (1973).

[44] I. N. Gyrbu, V. I. Ullyanov, and A. A. Botaki, Sov. Phys. Solid State **15**, 2252 (1974).

[45] S. Hart, J. Phys. D **1**, 1285 (1968).

[46] O. D. Slagel and H. A. McKinstry, J. Appl. Phys. **38**, 437 (1967).

[47] A. A. Botaki, I. N. Gyrbu, and A. V. Sharko, Sov. Phys. J. **15**, 917 (1972).

[48] M. Glyuas, F. D. Hughes, and B. W. James, J. Phys. C **8**, 171 (1970).

[49] J. J. Fontanella and D. E. Schuele, J. Phys. Chem. Solids **31**, 647 (1970).
[50] O. D. Slagel and H. A. McKinstry, J. Appl. Phys. **38**, 451 (1967).
[51] R. W. Roberts and S. S. Smith, J. Phys. Chem. Solids **31**, 619 (1970).
[52] G. R. Barsch and Z. P. Chang, in *Accurate Characterization of the High Pressure Environment* (Ref. 14), pp. 173–187.
[53] T. K. H. Barron, J. Phys. C **12**, L155 (1979).
[54] Y. Sumino and O. L. Anderson, in *CRC Handbook of the Physical Properties of Rocks*, edited by S. Carmichael (CRC Press, Boca Raton, FL, 1984), pp. 139–280.
[55] P. Vinet, J. Ferrante, J. H. Rose, and J. R. Smith, J. Geophys. Res. **92**, 9319 (1987).
[56] F. Birch, Phys. Rev. **71**, 809 (1947).
[57] W. B. Holzapfel, Rep. Prog. Phys. **59**, 29 (1996); Europhys. Lett. **16**, 67 (1991); High Press. Res. **7**, 290 (1991); J. Phys. Chem. Solids **55**, 711 (1994).
[58] M. Kumar and S. S. Bedi, J. Phys. Chem. Solids **57**, 133 (1996); L. M. Thomas and J. Shanker, Phys. Status Solidi B **181**, 387 (1994).
[59] J. R. Tessman, A. H. Kahn, and W. Shockley, Phys. Rev. **92**, 890 (1953).
[60] A. K. Koh, J. Phys. Chem. Solids **57**, 51 (1996).
[61] P. W. Bridgman, Proc. Am. Acad. Arts Sci. **76**, 1 (1945); E. A. Perez-Albuerne and H. G. Drickamer, J. Chem. Phys. **43**, 1381 (1965); L. Thomsen, J. Phys. Chem. Solids **31**, 2003 (1970); J. S. Weaver, T. Takahashi, and W. A. Bassett, in *Accurate Characterization of the High Pressure Environment* (Ref. 14), p. 326; J. N. Fritz, S. P. Marsh, W. J. Carter, and R. G. McQueen, *ibid.* pp. 201–208; R. Boehler and G. C. Kennedy, J. Phys. Chem. Solids. **41**, 517 (1980).
[62] N. Hamaya and S.-I. Akimoto, High Temp.-High Press. **13**, 347 (1981).
[63] D. R. Wilburn, W. A. Bassett, Y. Sato, and S. Akimoto, J. Geophys. Res. **83**, 3509 (1978).
[64] L. G. Liu and W. A. Bassett, J. Appl. Phys. **44**, 1475 (1973).
[65] L. Zhang and R. Boehler (unpublished).
[66] A. M. Hofmeister, in *Practical Guide to Infrared Microspectroscopy*, edited by H. J. Humecki (Dekker, New York, 1995), pp. 377–416.
[67] I. Jackson, H. Niesler, and D. Weidner, J. Geophys. Res. **86**, 3736 (1981).
[68] F. Birch, J. Geophys. Res. **83**, 1257 (1978).
[69] U. Köhler, P. G. Johannsen, and W. B. Holzapfel, J. Phys. C **9**, 5581 (1997).
[70] A. Navrotsky, Geophys. Res. Lett. **7**, 709 (1980).